ABSTRACT

LIBERA, DOMINIC A. Initial Studies Characterizing the Fate of Vomitus during a Projectile Vomiting Episode. (Under the direction of Dr. Francis de los Reyes and Dr. Lee-Ann Jaykus).

Human Noroviruses (HuNoVs) can cause severe vomiting to those who have been unlucky to be infected with it. The vomiting caused by this virus sheds millions of HuNoVs in the expelled vomitus. These HuNoVs can survive on surfaces and materials for long periods and can cause future outbreaks in high occupancy facilities like cruise ships. The fate of HuNoVs during projectile vomiting episodes must be examined to better understand how to prevent and clean up after outbreaks. A preliminary fate model was constructed to determine how much HuNoV ends up in three end states: airborne virus, virus splatter, and virus on the person vomiting. The fate model was also subjected to importance analysis to determine the main parameters that affect the preliminary fate model.

When vomitus is projectile vomited, it impacts the surrounding environment at a considerable speed thus creating a splattering affect. To characterize the furthest possible distance that vomitus could travel during a vomiting episode from splatter, a new experimental method named the "Tipping Bucket" experiment was designed. Two simulated vomitus matrices were used: reconstituted instant oatmeal (to simulate vomitus having high solids content) and artificial saliva (a dilute solution of porcine mucin in saline). Artificially colored vomitus with volumes ranging from 50-800 ml was dropped at a height of 3.5 ft. An image analysis program measured the furthest distance traveled by vomitus droplets. For oatmeal, the furthest distance traveled by a droplet was highly dependent upon volume, with the mean distance traveled ranging from 3-3.5 ft. for higher volumes ($\geq$600 ml). On the other hand, regardless of volume, artificial saliva experiments yielded a mean distance of 8-12 ft.;

the greatest distance traveled in any one experiment was 14.5 ft. These results can be used to suggest to high occupancy facility personnel that the recommended area for clean-up and disinfection should be at a 14.5 ft. radius from the vomiting episode location.

Aerosolization of HuNoV caused by vomiting would most likely extend the recommended area for disinfection far beyond 14.5 ft. especially in environments with constant air flow. To better characterize the phenomenon of virus aerosolization during vomiting, a simulated physical vomiting model was constructed using the theory of similitude. The simulated vomiting apparatus, which uses scaled pressures consistent with pressures observed inside the human abdominal cavity during vomiting, will be a realistic model that can be used to study virus transmission occurring as a consequence of aerosolization during vomiting. Future studies will use the vomiting model to study how environmental factors such a ventilation affect transmission of HuNoV and how long HuNoV can remain dispersed in the air with their infectivity intact.

Initial Studies Characterizing the Fate of Vomitus during a Projectile Vomiting Episode

by
Dominic Anthony Libera

A thesis submitted to the Graduate Faculty of
North Carolina State University
in partial fulfillment of the
requirements for the degree of
Master of Science

Environmental Engineering

Raleigh, North Carolina

2013

APPROVED BY:

_____	_____
Dr. Francis de los Reyes Committee Chair	Dr. Chris Frey
_____	
Dr. Lee-Ann Jaykus	

DEDICATION

To my Twin Sister Hannah, Brother Jacob, and Sister Theresa. Never doubt that you are smart enough to pursue higher education; we all have the seed of greatness in us. Believe in yourself and never give out, never give in, and never give up.

"Remus, are you next?"

BIOGRAPHY

Dominic Anthony Libera was born in Durham, NC on February 3rd, 1989 to Joseph Libera and Patricia Libera. He grew up in Elon, NC with Twin Sister Hannah, Brother Jacob, and Sister Theresa. Dominic attended North Carolina State University and received a Bachelor's of Science in Environmental Engineering in 2011. While enrolled, Dominic was a member of the Tau Beta Pi honor society, the Chi Epsilon honor society, and the University Scholars Program. At the present moment, Dominic is pursuing a Master's of Science in Environmental Engineering at North Carolina State University. Upon completion of his master's program he will continue his education at the university and pursue a Doctorate in Civil Engineering studying hydrology.

ACKNOWLEDGMENTS

I would like to thank my Mother and Father for always encouraging me and for strengthening my will to succeed; I can always count on your love to calm and comfort me.

I would like to thank my Brother and Sisters for giving me love and support during difficult times.

I would like to thank Dr. de los Reyes for his invaluable advice and mentorship throughout my Master's degree.

I would like to thank my colleague Grace Tung for her assistance in all of my work; it would not have been possible without her.

I would like to thank Dr. Jaykus and her Food Science Lab for all of their advice and support.

I would like to thank David Black for always taking time out of his busy schedule to help me around the lab.

I would like to thank Jake Rhoads for his help and expertise in the field of fabrication.

I would like to thank everyone from my graduate student office; each day they remind me of how much fun graduate school can be.

I would like to thank Dr. Kenneth Koch from The Wake Forest School of Medicine, for his consultation on vomiting.

This project was supported by Agriculture and Food Research Initiative Competitive Grant no. 2011-68003-30395 from the USDA National Institute of Food and Agriculture.

TABLE OF CONTENTS

LIST OF TABLES vi
LIST OF FIGURES vii
CHAPTER 1: INTRODUCTION 1
Norovirus Background 1
Research Objectives 1
Vomiting Physiology 2
Dimensions of the Human Body 6
Expert Consultation 8
Vomiting Pressure 9
CHAPTER 2: BUILDING A PRELIMINARY FATE MODEL 11
Introduction 11
Methods and Materials 12
Factors that Affect Vomiting 13
Factors that Affect Coughing, A Proxy for Vomiting 14
Results and Discussion 18
Conclusions 22
CHAPTER 3: QUANTIFYING VOMITUS SPLATTER 24
Introduction 24
Methods and Materials 24
Experimental Design 24
Experimentation with Simulated Vomitus 27
Results and Discussion 28
Conclusions 37
CHAPTER 4: DEVELOPING A VOMITING MACHINE MODEL 39
Introduction 39
Methods and Materials 39
Similitude Overview 39
Determining π Groups 41
Achieving Similitude 45
Model Construction 48
Vomitus, Piston, and Pressure Scaling 50
Containment Chamber Design 52
Results and Discussion 56
Using the Containment Chamber and Biosampler 59
Conclusions 62
CHAPTER 5: CONCLUSIONS AND RECOMMENDATIONS 64
Conclusions 64
Recommendations 66
REFERENCES 68

LIST OF TABLES

Table 1. Summarized table of esophagus and mouth dimensions in cm and in 8
Table 2. List of Inputs for the Analytica Model 16
Table 3. Machine Model Parameter Dimensions..... 46
Table 4. Typical volumes of vomitus and air that could be observed during a vomiting episode 50
Table 5. Scaled down volume sizes for the vomiting machine model..... 51
Table 6. Scaled stomach chamber pressures..... 51
Table 7. Piston lengths corresponding to the total chamber volumes..... 52

LIST OF FIGURES

Figure 1. Close up of the human stomach showing the pylorus, lower esophageal sphincter, and fundus region 3
Figure 2. Diagram of the upper gastrointestinal tract complete with mouth, esophagus and stomach 5
Figure 3. The larynx and the pharynx (includes the laryngopharynx, oropharynx, nasopharynx). 6
Figure 4. Diagram of Analytica Model 16
Figure 5. Distribution of the amount of HuNoV in the air after a vomiting episode 18
Figure 6. Distribution of the amount of HuNoV in vomitus splatter after a vomiting episode 19
Figure 7. Important analysis results when making "Airborne Virus" the importance node 20
Figure 8. Important analysis results when making "Virus in Vomit Splatter" the importance node 21
Figure 9. Distribution of the number of airborne viruses when changing the virus concentration to have a mean of $1x10^{10}$ 21
Figure 10. Tarp Target 26
Figure 11. Tipping Bucket Experimental set-up 26
Figure 12. Break bar 28
Figure 13. Example of artificial saliva splatter pattern (Trial 5, 600ml) 29
Figure 14. Oatmeal Trial 1 30
Figure 15. Oatmeal Trial 2 31
Figure 16. Oatmeal Trial 3 32
Figure 17. Oatmeal Trial 4 33
Figure 18. Oatmeal Trial 5 34
Figure 19. Surface area covered by oatmeal splatter (average values appear as dots and error bars represent minimum and maximum values) 35
Figure 20. Furthest distances traveled by droplets in oatmeal trials 36
Figure 21. Furthest distances traveled by droplets during saliva trials 37
Figure 22. Diagram of fluid flow in (a) human body and (b) scaled model 41
Figure 23. Diagram of vomiting device model 49
Figure 24. Air chamber dimensions 54
Figure 25. Diagram of the SKC Biosampler 55
Figure 26. Vomiting device housed inside air chamber 56
Figure 27. Picture of the vomiting device attached to the air chamber 57
Figure 28. Picture of the vomiting machine simulating a vomiting episode right as the surrogate vomitus exits the mouth 58
Figure 29. Picture of the inside of the air chamber after a simulation of vomiting 58
Figure 30. Free body diagram showing the forces acting on a settling particle 60

CHAPTER 1: INTRODUCTION

Norovirus Background

Human noroviruses (HuNoVs) cause an estimated 5.5 million cases of foodborne gastrointestinal disease in the United States annually and account for up to 50% of all foodborne disease outbreaks (Scallan et al., 2011). Cases of HuNov are characterized by nausea, acute on-set vomiting and watery diarrhea. Symptoms can last up to 1-3 days before they cease. Their low infectious dose (~10-20 infectious particles) and lengthy environmental persistence contribute to their high degree of transmissibility (CDC, 2011). These characteristics of the HuNov put high occupancy environments with food services such as daycares, elderly care facilities, restaurants, and cruise ships at a high risk for HuNoV outbreaks (Baker et al., 2011, Lopman et al., 2004, Widdowson et al., 2004).

People can become exposed to HuNoV through direct contact with HuNoV related vomitus and fecal matter, contact with people infected with HuNov (e.g. hand contact) and contact with HuNoV contaminated surfaces. Millions of viruses are also shed in vomitus and epidemiological evidence suggests that they are transmitted through aerosol formation during vomiting (Marks et al., 2000; Lopman et al., 2012). If vomitus is not properly cleaned up and disinfected from exposed environments, it can pose a threat to a HuNov outbreak.

Research Objectives

The importance of vomitus in foodborne transmission of HuNoV is currently unknown. Managing vomiting incidents in food service is a major concern of retailers

(Mokhtari & Jaykus, 2009). Some cleaning guidelines for vomiting incidents have been produced by The Food Marketing Institute (FMI) and The Centers for Disease Control and Prevention (CDC), but there is little scientific data upon which to base these guidelines (CDC, 2013, FMI, 2010). The FMI reports that past outbreaks suggest that HuNoV could contaminate environmental surfaces up to 25 feet away (FMI, 2010). The first objective of this study was to characterize the radius of impact of a simulated vomiting event, i.e. how far can vomitus travel from the initial vomiting location, for the purposes of improving clean-up and disinfection guidelines. The second objective of this study was to provide the details for production of a simulated vomiting device that will eventually be used to further characterize HuNoV spread as a consequence of vomiting.

Vomiting Physiology

Vomiting is the forceful expulsion of food out of the mouth, which is different from retching and regurgitation. Retching is the rhythmic reverse peristaltic activity of the esophagus and stomach accompanied by exhaling respiratory movements that precede vomiting. Although retching may feel like vomiting, retching is strictly dry and has no expulsion of vomitus. Regurgitation is simply when a small amount of stomach contents reflux back into the mouth (Keshav, 2004).

Intensive studies on the physiological characteristics of vomiting have been examined on animals rather than humans (Lumsden & Holden, 1969). The responses of the laryngeal, pharyngeal, and hyoid muscles during each stage of vomiting processes in canine subjects was studied (Lang et al., 2002). Vomiting has three stages: pre-retch, retch, and vomitus

expulsion. During the pre-retch stage, the posture of the dogs changed as they extended their necks and lowered their heads in preparation for retching and vomiting (Lang, Dana, Medda, & Shaker, 2002)).

Retching culminates in a powerful sustained contraction of the abdominal muscles accompanied by the descent of the diaphragm. This movement helps increase the intragastric pressure in a human stomach to accelerate the gastric contents up to the mouth at a considerable speed (Lumsden & Holden, 1969). The average number of retches per vomiting episode is 10 ± 1 (Lang et al., 2002).

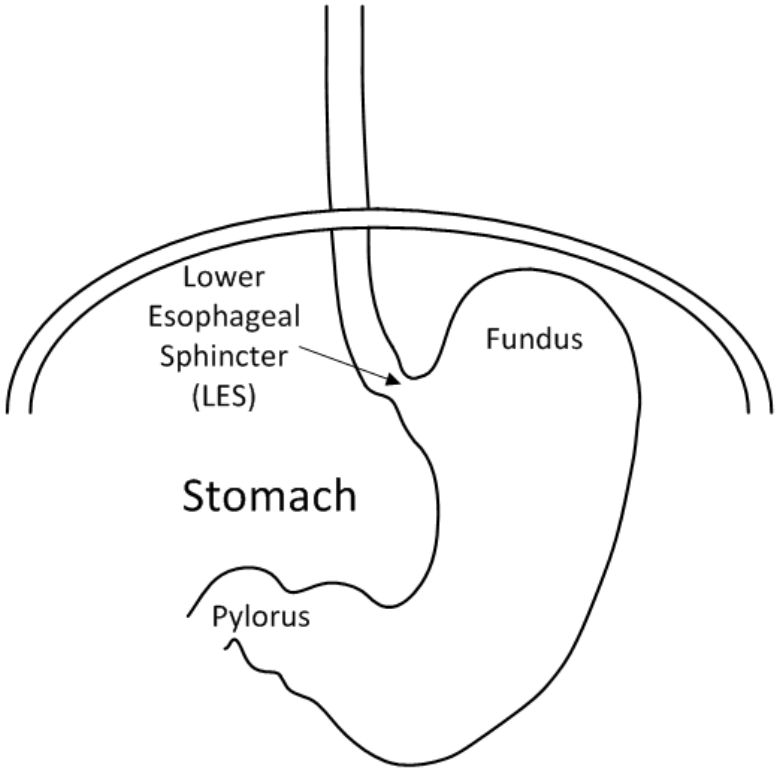

Figure 1. Close up of the human stomach showing the pylorus, lower esophageal sphincter, and fundus region

During vomiting the abdominal muscles, including the diaphragm, continue to contract, further increasing the intra-abdominal and intrathoracic pressure, the pressure inside the chest. The primary motive force (i.e. the force causing motion) for vomitus expulsion is the pressure gradient between the stomach and esophagus generated by diaphragmatic and abdominal muscle compression with a closed pylorus, shown in Figure 1. This pressure helps empty stomach contents into the upper gastrointestinal tract, as shown in Figure 2, (Keshav, 2004). During the first part of vomiting, stomach contents are transported by forceful expulsion from the stomach through the maximally relaxed lower esophageal sphincter, seen in Figure 1 (Lang et al., 2002). Simultaneously, the epiglottis shuts off the larynx, which is drawn forwards by muscles in the jaw and neck, seen in Figure 3. The soft palate is drawn upwards, closing off the nasopharynx; these coordinated muscular movements protect the airway as vomitus is expelled (Keshav, 2004). Additionally, the muscles in the pharynx are activated to begin dilation of the upper throat (Lang et al., 2002).

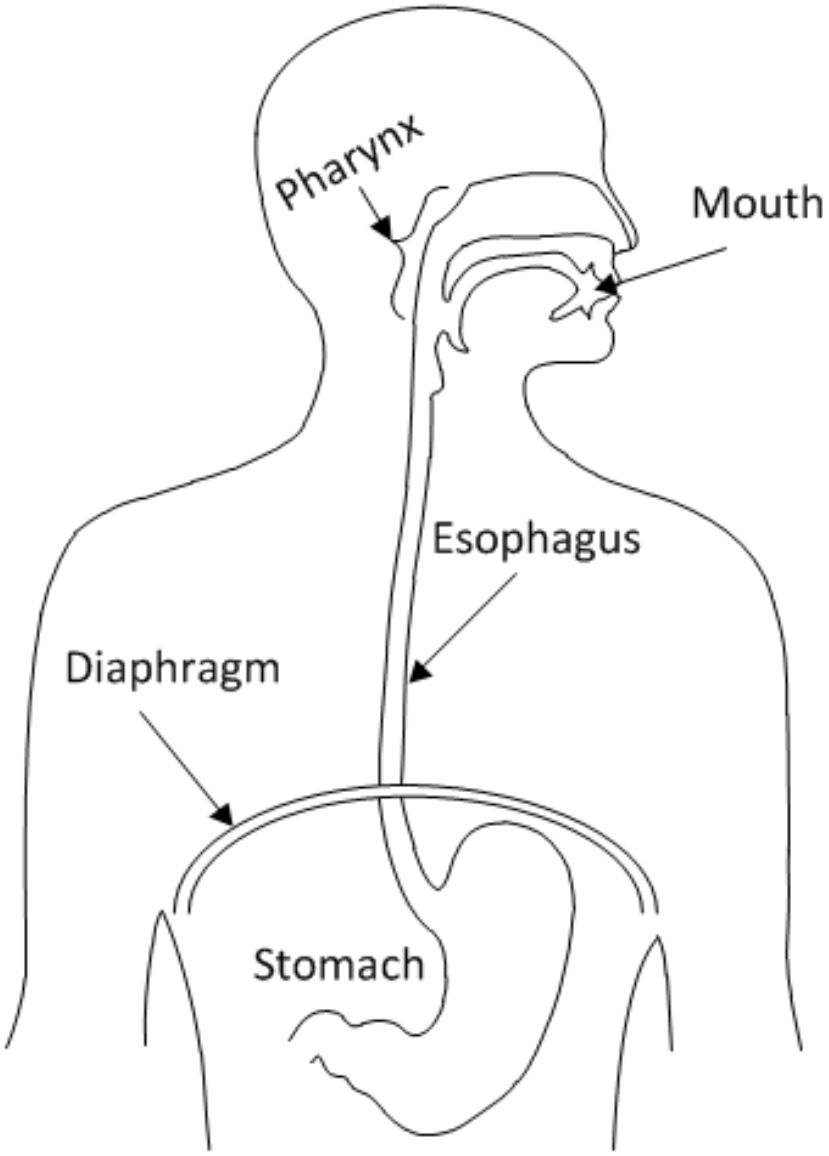

Figure 2. Diagram of the upper gastrointestinal tract complete with mouth, esophagus and stomach

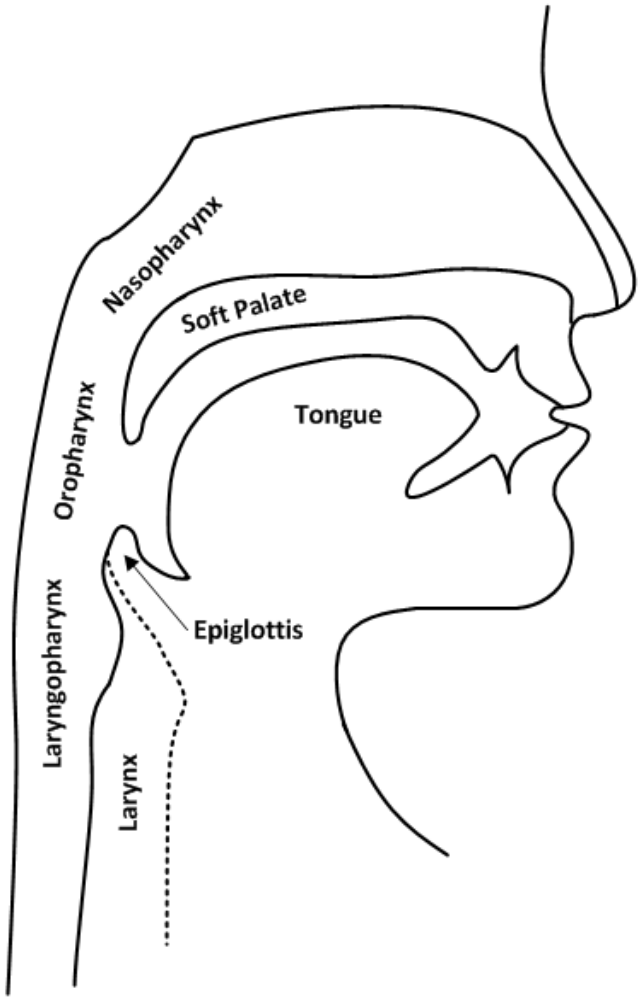

Figure 3. The larynx and the pharynx (includes the laryngopharynx, oropharynx, nasopharynx).

Dimensions of the Human Body

To construct a vomiting device model of the human upper gastrointestinal tract, the dimensions of certain human components must be parameterized. Components of the human upper gastrointestinal tract that were included in the scaled model are the mouth, the esophagus, and the stomach. The human stomach changes size and shape depending on the

amount of recently consumed food. In addition, the human stomach does not have a uniform shape; these characteristics make it hard to find a measurement that would represent the average stomach size.

This section will parameterize only the lengths and diameters of the human esophagus and mouth. The length of the human esophagus ranges from 23 to 25 cm; for the purposes of this study 25 cm will be used (Korn et al., 2003, Kuo, 2006). Also, the diameter of the esophagus can be between 2 and 3 cm; for this study 2.5 cm will be used (Kuo, 2006). A case study looking at the maximum distance of the mouth opening, measured as the maximal inter-incisal distance, found that the average mouth opening to be 5.72 cm (Dijkstra, Hof, Stegenga, & De Bont, 1999). To construct the simulated vomiting device, the shape of the human mouth was treated as a length of circular tubing; the maximum distance of the mouth opening was used as the diameter of the circular tubing. The length of a human mouth, the distance from the front of the mouth to the back of the throat, was difficult to find in the literature. In this study the mandibular length was used as substitute for mouth length. The mandibular length is the measurement from the lower incisors to mandibular condyle, the upper tip of the jaw bone which connects to the skull behind the ears. The case study looking at mouth opening distances also measured mandibular length; the average mandibular length reported was 9.7 cm (Dijkstra et al., 1999). A summary of the component parameters are shown in Table 1; both metric and SI units are listed.

Table 1. Summarized table of esophagus and mouth dimensions in cm and in

Human Body Dimensions		
	(in)	(cm)
Esophagus Lenth	9.843	25
Esophagus Diameter	0.984	2.5
Mouth Length	3.54	9.7
Mouth Diameter	2.25	5.72

Expert Consultation

There is very little information on the topic of vomiting with respect to spread of infectious agents. In an effort to better understand the physiology of vomiting, Dr. Kenneth Koch, Wake Forest School of Medicine, a leading expert in the field of gastroenterology was consulted. Two one-hour interviews were conducted; the first on November 11th, 2011 and the second on January 7th, 2013. The first interview concentrated on determining the maximum amount of vomitus that could be projected during a single vomiting episode, and typical volumes and viscosities of vomitus. According to the expert, volumes of vomitus could vary depending on the person's height, weight, and diet. Considering these variations, 800 ml of vomitus in a single vomiting episode would be considered a typical maximum. Vomitus volumes below 50 ml would not be typical during a projectile vomiting episode. The expert advised that the viscosities of vomitus will range depending on the solids content of the stomach contents. Vomitus with high solids contents would be thick with food particles; reconstituted instant oatmeal was used as a surrogate for high solids content

vomitus. Vomitus with low solids contents would be very thin and watery; simulated saliva was used as a surrogate for low solids content vomitus.

The second interview focused on identifying important physiological characteristics to consider in building a simulated vomiting device. The expert provided some significant information regarding key parameters that needed to be considered in design of the device.

One key suggestion made by the expert was that there is about 50-100 ml, at minimum, of air in the fundus region of the stomach, which could theoretically contribute to some degree of vomitus aerosolization during vomiting. Secondly, it takes about 15- 40 mmHg (0.77 psi) of pressure to blow open the lower esophageal sphincter (LES); pressures greater than this will most likely produce projectile vomiting. Lastly, when vomiting, a person's neck is extended with the mouth pointed towards the ground; this extension creates a smoother angle for vomitus flow. The expert also noted that conserving the size and shape of the stomach in the vomiting model design is not necessary for purposes of examining bioaerosolization, as long as the model uses the lengths and diameters of the human mouth and esophagus (Kenneth Koch, 2011).

Vomiting Pressure

Since the pressure build up inside the stomach is the main force in projectile vomiting, the importance of knowing the range of pressures observable inside the stomach is crucial to model design. A recent study quantified the intragastric and intravascular pressures through the use of manometry catheters. Researchers monitored the intragastric pressure of ten individuals during periods of rest, coughing, bench pressing, and induced

vomiting. A manometry catheter was inserted through the nose and secured inside the stomach inside the fundus region, the top area of the stomach, shown in Figure 1. Volunteers drank 250 ml of water, followed by 30 ml of Ipecac syrup, and another 240 ml of water. Volunteers laid on their right sides while the continuous measurements were recorded during vomiting. Episodes of vomiting were distinguished from retches or dry heaving. If the volunteer did not vomit within 30 minutes another 15 ml of Ipecac syrup was ingested. Continuous measurements were taken during vomiting. The highest intragastric pressure observed was 290 mmHg which corresponds to 5.6 psi. The mean intragastric pressure during vomiting was 82 mmHg which corresponds to 1.6 psi (Iqbal et al., 2008).

CHAPTER 2: BUILDING A PRELIMINARY FATE MODEL

Introduction

The HuNoV is a highly contagious virus that has been recalcitrant to various control measures in the food service environment. HuNoV related vomiting episodes in a food preparation environment can potentially contaminate food (Cheesbrough et al., 2000). Food can also be contaminated with HuNoV from food handlers during food preparation; in response an exposure model describing the transmission of HuNoV from food handlers to food during food preparation was published (Mokhtari & Jaykus, 2009). There is a lack of knowledge on what actually happens to HuNoV when it exits a human during a vomiting episode. Understanding the fate of HuNoV during a vomiting episode is extremely important to the food industry in protecting people from foodborne diseases by directing proper clean up, disinfection, and quarantine guidelines. A fate model quantifying the amount of HuNoV transported from the human body specifically by vomiting to the environment can aid in the prevention and management of outbreaks in high occupancy environments.

In the first part of this chapter, important factors that affect the number of HuNoV particles that leave the human during vomiting were summarized in a literature review. Secondly, Analytica was used to construct a preliminary fate model to determine how much HuNoV partitions in three end states: airborne virus, virus splatter, and virus on the person vomiting. Analytica is visual software developed by Lumina Decision Systems for analyzing decision models in the form of influence diagrams. In addition, an importance analysis was

done to determine which key inputs the variability in both virus splatter and airborne virus are most sensitive.

Methods and Materials

A stochastic model was built using Analytica Version 4.4 to predict the amount of HuNoV present in three states after a vomiting episode:

1. HuNoV suspended in the air (airborne virus)
2. HuNoV suspended in vomitus splattered on the environment or other people
3. HuNoV suspended in vomitus splattered on the individual vomiting

Three states were chosen to make the model simple and easy to understand. These states were found by examining arbitrary realistic vomiting scenarios, and choosing three simple states that could encompass all of the states of vomitus in the scenarios.

Studies examining the airborne transmission of HuNoV during vomiting are scant and currently there is very little data quantifying if and how much virus can be aerosolized during vomiting. The purpose of this modeling exercise was to develop a preliminary model that could later be updated to include results from future studies to understand the dynamics of vomiting and associated virus aerosolization. Since there are no published studies that report on the size and amount of aerosolized virus particles caused from just vomiting, this model does not use vomiting as the mechanism for aerosolizing viruses. Instead, the coughing associated with hacking up excess mucus in the throat and oropharynx was used as a proxy for virus aerosolization after a vomiting event.

Factors that Affect Vomiting

Little is known about the myriad factors that impact vomiting. A key unknown factor is the concentration of HuNoV in vomitus. One study reports that the concentration of HuNoV can be up to 10^5 viruses per milliliter of vomitus during a vomiting episode. Because there is so little data, developing a distribution of virus concentration in vomitus is difficult (Johnson, Lynch, Marshall, Mead, & Hirst, 2013). A lognormal distribution with a mean of $1x10^6$ and a standard deviation of 1,000 was arbitrarily adopted for the HuNoV concentration in vomitus in the absence of distribution data.

A typical human stomach can hold up to four liters of contents but total stomach contents are not emptied during one vomiting episode. It takes multiple vomiting episodes to empty a stomach with vomit volumes ranging from between 50 ml to 800 ml per episode. It is equally likely that any of these volumes could be expelled during any single vomiting episode (Kenneth Koch, 2011). A uniform distribution ranging from 50 ml to 800 ml was used for representing the volume of vomitus. When a person experiences a vomiting episode there is a possibility that vomitus could end up on the person's body or clothes. For the purpose of this project the volume of vomitus that can end up on a person while vomiting has been assigned as a uniform distribution ranging from 0 to 100 ml. These were determined by assuming that anything greater than 100 ml would quickly drip of a person and end up as vomitus splatter.

Factors that Affect Coughing, A Proxy for Vomiting

Immediately after vomiting, vomitus coats the upper throat area including the tongue, tonsils and oropharynx (back of the throat) (Morawska, 2006). The human body naturally exerts droplets of saliva from the mouth and throat during common expiratory activities such as talking, breathing and coughing (Duguid, 1945). Theoretically, coughing directly after a vomiting episode could aerosolize HuNoV, coating the mouth and throat. Following a vomiting episode, an infected person can experience multiple coughs or retches, known as dry heaving (Lang et al., 2002). Based on personal judgment from Dominic Libera, the number of coughs a person experiences during one vomiting episode has a triangle distribution with a minimum of 1, a maximum of 8, and a mean of 4 coughs; judgment was supported by reviewing video clips of people vomiting uploaded to a video-sharing website. These coughing and retching episodes are described as "throat only coughs," meaning that the mouth is fully dilated with the tongue depressed. During these "throat only coughs", virus coating the throat and mouth is formed into droplets by a process known as atomization. Atomization occurs when a high speed column or air is passed over a liquid body which physically pulls a small amount of liquid from the body. First a thin strand of liquid is formed and then split apart into many droplets that are carried off by the column of air (Duguid, 1945). Atomization forms two kinds of droplets: large droplets and droplet-nuclei (Morawska et al., 2006). Large droplets range in size from 100 microns to 500 microns that are too big to remain airborne (Papineni & Rosenthal, 1997). Large droplets fall immediately to the ground and land in the environment. For the purposes of this study, large droplets will be classified as existing as vomitus splatter after vomiting (Duguid, 1945).

Droplet-nuclei are smaller than 100 microns and can be as small as a couple of microns. AuvTool, a distribution fitting software, was used to fit a lognormal distribution to the data sets for the size of droplet-nuclei from a study done by JP Duguid (1946). Using the method of matching moments, a lognormal distribution was also fit to a data set (Nuguid, 1945) of the number of droplet-nuclei.

An influence diagram of the stochastic model built in Analytica is shown in Figure 4. The oval shaped nodes represent model inputs and are represented as distributions, or in the cases of the "Volume of Vomitus Splatter" node and the "Volume of Airborne Virus", are represented as a formulation of other inputs; the formulations can be found in Equations (2.1) and (2.2). The blocked nodes represent the three end states of HuNoV after a vomiting episode and are determined by performing numerical operations on the oval input nodes; formulations can be found in Equations (2.3), (2.4), and (2.5). Arrows show that an input node was used to calculate a blocked node or in some cases another input node. A summary of the input distributions and their corresponding sources is shown in Table 2.

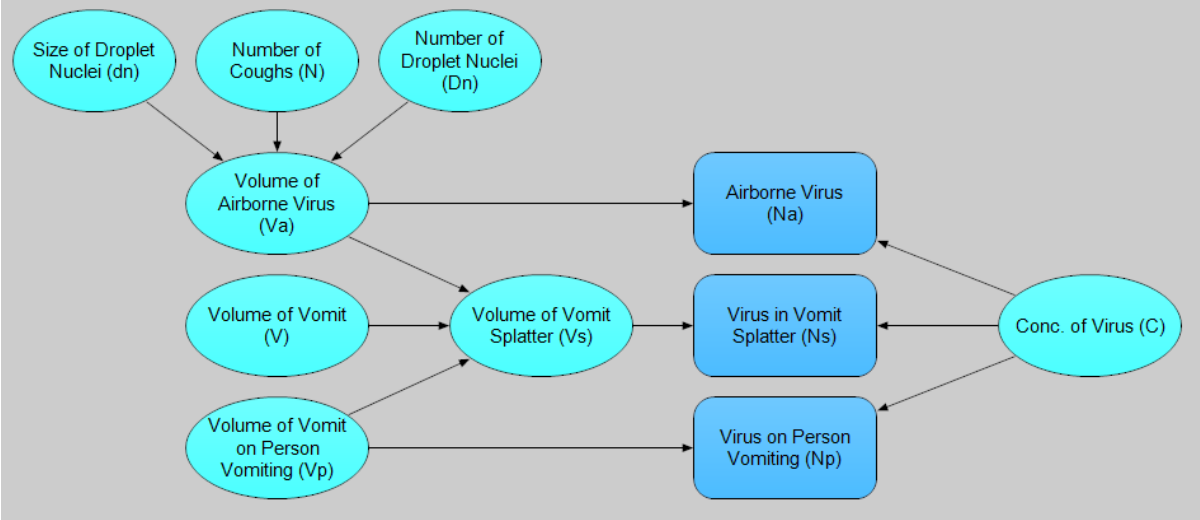

Figure 4. Diagram of Analytica Model

Table 2. List of Inputs for the Analytica Model

Parameter	Min	Max	Mean	Std. Dev.	Distribution	Source
Volume of vomitus (ml)	50	800	-	-	Uniform	(Koch 2011)
Volume of vomitus on patient (ml)	0	100	-	-	Uniform	Assumed
Concentration of virus (virus/ml)	-	-	1E+06	1000	Lognormal	Assumed
Number of coughs/retch	1	8	4	-	Triangle	Assumed
Size of droplet nuclei (µm)	-	-	2.76	0.86	Lognormal	(Duguid 1946)
Number droplet nuclei	-	-	8	1	Lognormal	(Duguid 1945)

The equations listed below were used in determining the three blocked nodes and some of the oval nodes shown in Figure 4:

$$V_A = \frac{1}{6} \cdot \pi \cdot d_n^3 \cdot 1x10^{-12} \cdot N \cdot D_n \tag{2.1}$$

$$V_s = V - V_A - V_P \tag{2.2}$$

$$N_A = C \cdot V_A \tag{2.3}$$

$$N_p = C \cdot V_P \tag{2.4}$$

$$N_S = C \cdot V_S \tag{2.5}$$

Where:

$V = volume\ of\ total\ vomitus\ (ml)$
$V_A = volume\ of\ airborne\ vomitus\ (ml)$
$V_S = volume\ of\ vomitus\ splatter\ (ml)$
$V_p = volume\ of\ vomit\ on\ patient\ (ml)$
$N_A = number\ of\ airborne\ viruses$
$N_P = number\ of\ viruses\ on\ patient$
$N_S = number\ of\ viruses\ in\ vomit\ splatter$
$C = concentration\ of\ virus\ in\ vomitus\left(\frac{virus}{ml}\right)$
$N = number\ of\ coughs$
$d_n = size\ of\ droplet\ nuclei\ (\mu m)$
$D_n = number\ of\ droplet\ nuclei$

Using Analytica, an importance analysis was run on the "Virus in Vomit Splatter" node and "Airborne Virus" node to determine which key inputs contributed the most to the variability in the output. An importance analysis in Analytica is when a certain node is classified as "Important", this is done by editing the properties of the node, which means it takes all of the inputs into that node and performs a rank-order correlation between the distribution of the importance node and the distributions of the input nodes. The ranks range from 0 to 1; a value of 1 is the highest correlation, meaning that all of the variability in the importance node is explained by the variability in the input node.

Results and Discussion

Figure 5 shows the distribution of the amount of HuNoV remaining in the air after a vomiting episode; recall in this model that the airborne virus is aerosolized solely by coughing or retching. The results in Figure 5 show that there is a 95% probability that the number of airborne viruses will be less than or equal to $2x10^{-3}$ suggesting that there is no aerosolization. Figure 6 shows the distribution of the amount of HuNoV existing in vomitus splatter after a vomiting episode. There is a 95% probability that the number of viruses in vomitus splatter will be less than or equal to $7.5x10^{8}$. Currently the model results show that the majority of virus particles end up in vomitus splatter.

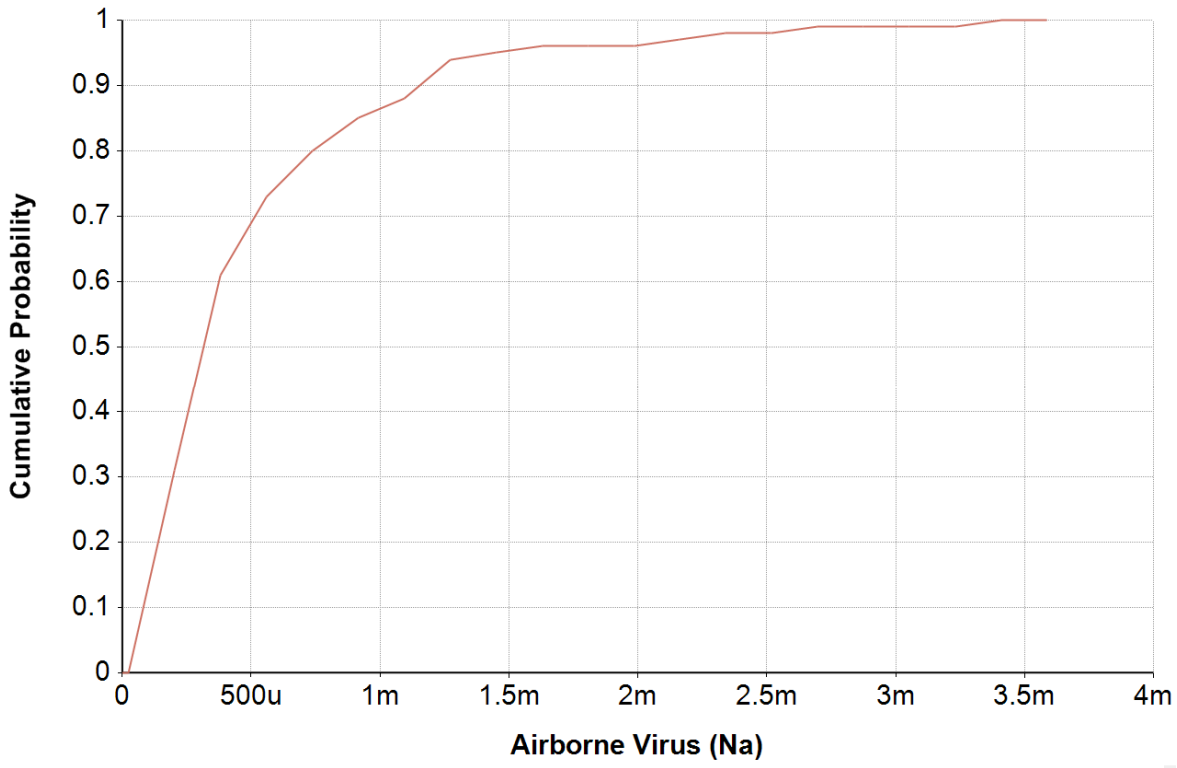

Figure 5. Distribution of the amount of HuNoV in the air after a vomiting episode

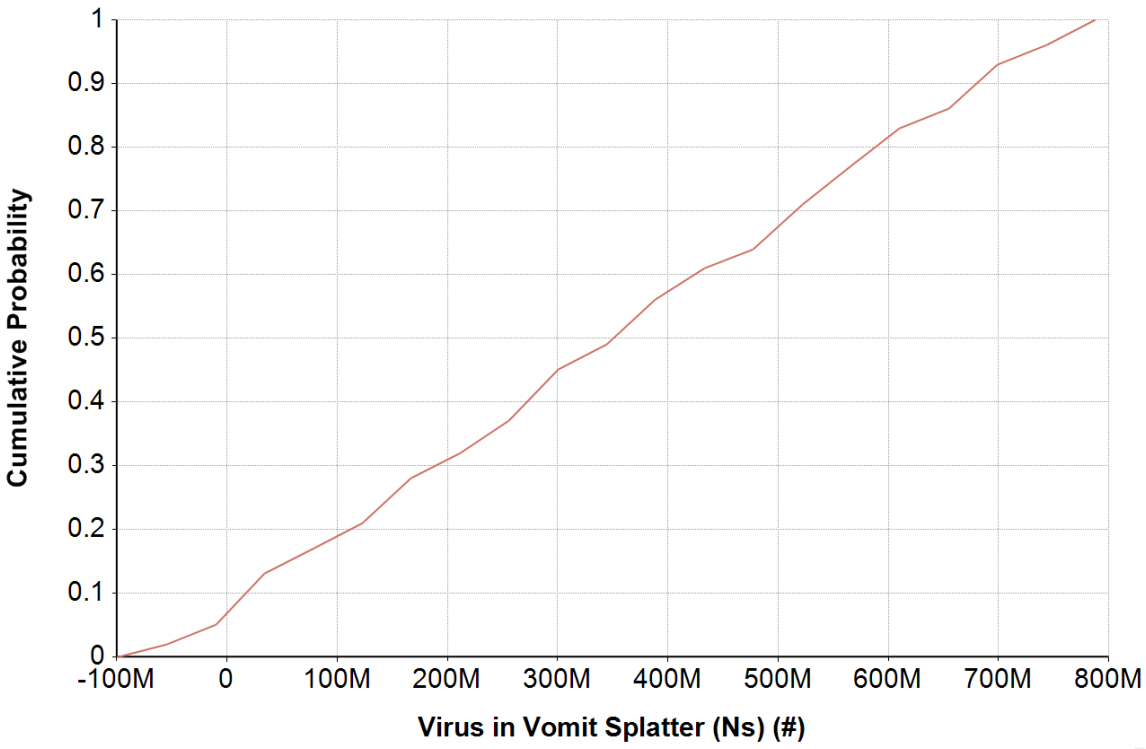

Figure 6. Distribution of the amount of HuNoV in vomitus splatter after a vomiting episode

Figure 7 shows the results from the Importance Analysis when making "Airborne Virus" the importance node. The results show that the variability in the number of airborne viruses can be explained by the variability of the volume of airborne virus; this is to be expected because all of the inputs are first used in calculating the volume of airborne virus node then the volume of airborne virus node is used to calculate the number of airborne viruses. Looking at the other input nodes, size of droplet nuclei shows an importance of over 0.9, indicating that the distribution of the amount of airborne viruses is very sensitive to the distribution of the size of droplet nuclei.

Figure 8 shows the results from the Importance Analysis when making “Virus in Vomitus Splatter” the importance node. The results show that the distribution of the number of viruses in vomitus splatter is most sensitive to the distribution of volume of vomitus splatter. Just as before, this was expected because the volume of vomitus splatter node uses all of the other oval nodes as inputs. The second most important input is volume of vomitus, with an importance of about 0.99, indicating that the distribution of the number of viruses in vomitus splatter is very sensitive to the distribution of total vomitus volume.

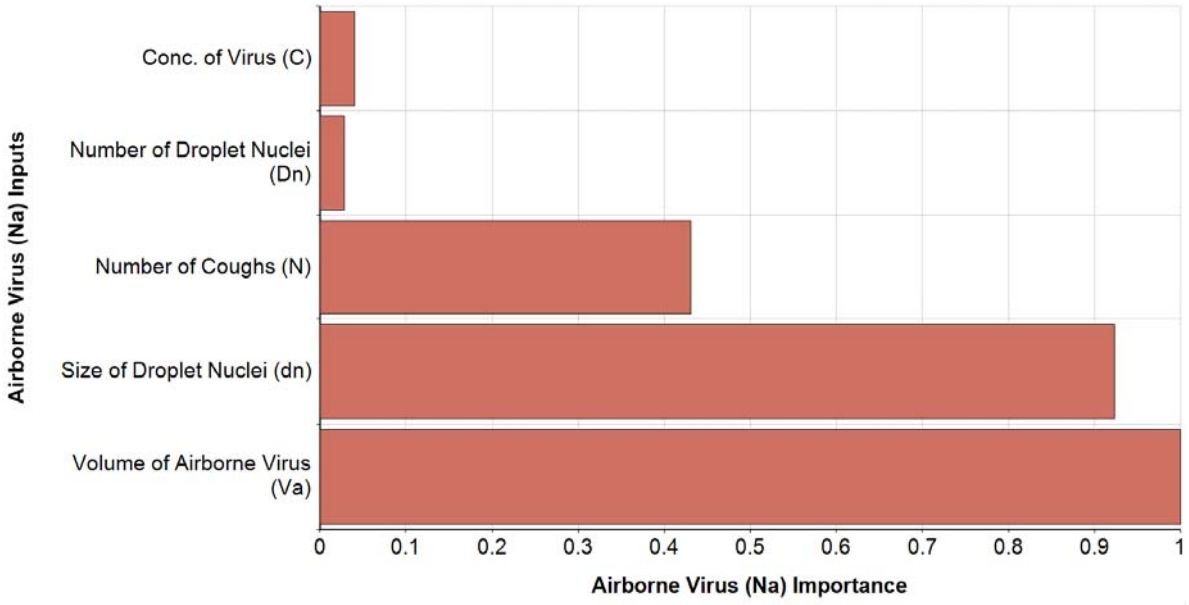

Figure 7. Important analysis results when making "Airborne Virus" the importance node

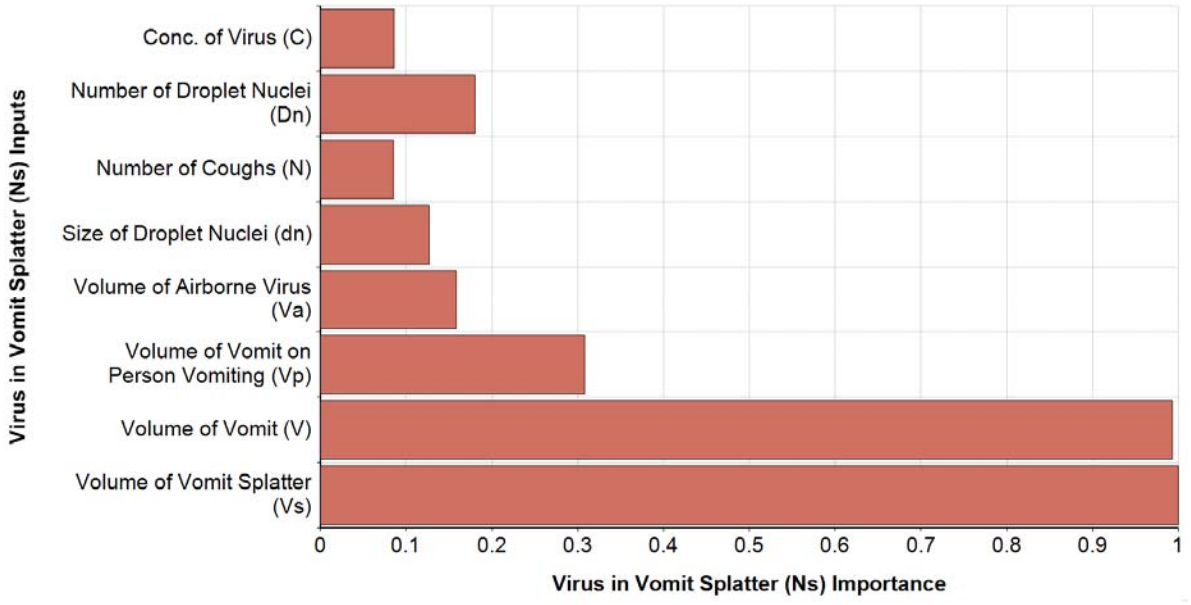

Figure 8. Important analysis results when making "Virus in Vomit Splatter" the importance node

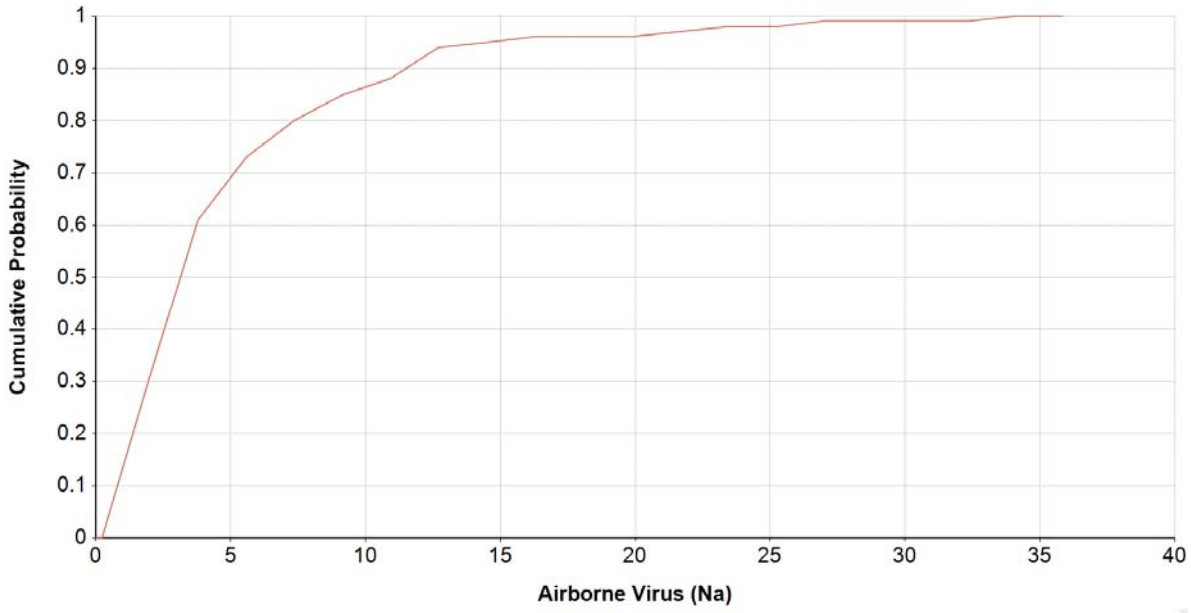

Figure 9. Distribution of the number of airborne viruses when changing the virus concentration to have a mean of $1x10^{10}$

As mentioned previously, the concentration of HuNoV in vomitus is not well characterized. The distribution of the number of airborne viruses, when the concentration distribution was changed to have a mean value of $1x10^{10}$ and a standard deviation of 1,000 (Figure 9), shows a 95% probability that the number of airborne viruses will be less than or equal to 20.

Conclusions

Importance analyses can provide information on which input distributions are the most important in determining an output distribution. Using this information, further research can be performed to better characterize the important input distributions. For example, characterizing the distribution of the size of droplet nuclei could improve estimates of the distribution of airborne viruses. Also, better characterization of the total volume of vomitus could improve estimates of the distribution of viruses in vomitus splatter. Improving the characterization of virus concentration in vomitus could drastically improve the entire model because when a low mean virus concentration is used there are not any aerosolized viruses but when a high mean virus concentration is used there are just enough aerosolized viruses to get a person sick. The results from Figure 5 did not provide any useful information in terms of how many viruses can be airborne, but Figure 9 showed a 95% probability that there will be less than or equal to 20 viruses in the air. This information is useful because the infectious dose of HuNoV is 10 to 20 infectious viruses (CDC, 2011).

This is a preliminary model and the main purpose of its construction was to serve as an infrastructure for future models. When better data become available, the model can be updated to include vomiting as a mechanism for virus aerosolization.

CHAPTER 3: QUANTIFYING VOMITUS SPLATTER

Introduction

Persons infected with NoV shed millions of viruses suspended in vomitus during a single vomiting episode (Caul, 1994). When vomitus impacts surrounding surfaces it creates a splattering effect that further dissipates vomitus droplets. HuNoVs are relatively stable in the environment and can survive in severe conditions (CDC, 2011). Proper disinfection of surrounding environments in high occupancy facilities (e.g. nursing homes, cruise ships) after a vomiting episode is crucial to prevent further NoV cases. Some protocols for clean-up and disinfection have been published by the CDC, but little is known about how far vomitus splatter can travel during vomiting (CDC, 2013). Guidelines that lack a metric for determining the contamination area from vomiting incidents makes it difficult for facility personnel to target all of the contaminated surfaces. The goal of this chapter is to characterize how far vomitus can splatter during a vomiting episode to improve environmental disinfection guidelines.

Methods and Materials

Experimental Design

There is no known methodology for characterizing the radius of impact of vomitus during a vomiting episode. A new method named the "Tipping Bucket" experiment was designed to determine the maximum distances traveled by vomitus droplets during a singular vomiting episode. The simulation involved pouring simulated vomitus onto a white tarp

target. The tarp was covered with a target design created from black electrical tape as shown in Figure 10. The target has rings one foot apart with the center marked with a "+" symbol. A step ladder was placed on top of the tarp and a bucket platform 3.5 feet above ground level was attached by a C-clamp to one of the ladder's steps. This height was used to simulate a bent over person experiencing a vomiting episode. Resting on the platform was a plastic one liter bucket with a hinge connecting the bottom of the container to the platform. Large rolls of translucent paper were tapped together and placed over the tarp target; the electrical tape target was still visible through the white paper. Paper rolls were used to make clean-up quick and easy between experiment trials. A hollow PVC pipe arm was arranged on the top of the ladder by sliding two perpendicular supporting pipes into corresponding holes at the top of the ladder's cap, as shown in Figure 11. Inside the PVC pipe arm was a monopod secured by two screws. Attached to the end of the monopod was a Canon EOS Rebel T2i® digital camera with a bubble level to create an orthogonal angle to the tarp target. Camera settings were changed to remote control capturing. Two simulated vomitus matrices were used in the experiment: reconstituted instant oatmeal and artificial saliva. Food coloring was added to each matrix to increase the contrast against the white tarp. Instant oatmeal was chosen to represent vomitus with high solids content. Artificial saliva, a solution of porcine mucin, water, and sodium chloride was used to represent vomitus with low solids content. Dr. Kenneth Koch, Wake Forest Baptist Medical Center, suggested these two matrices will represent the upper and lower bounds of possible vomitus viscosities. Viscosities of each matrix were measured using a Brookfield digital viscometer, model DV-E.

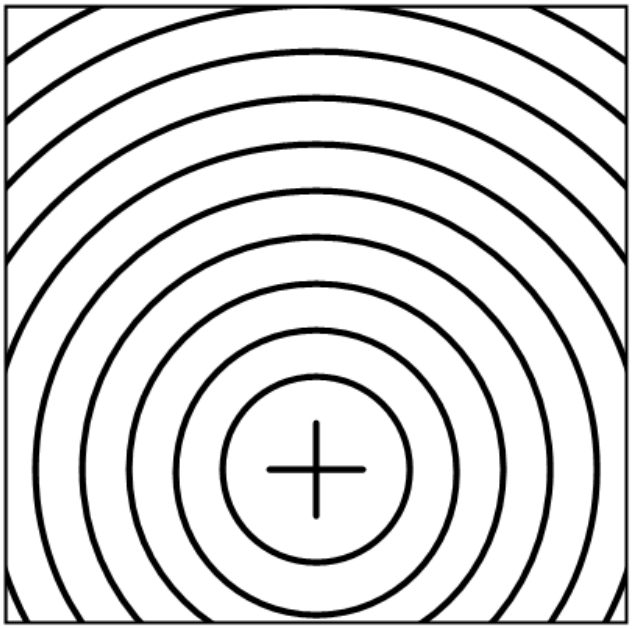

Figure 10. Tarp Target

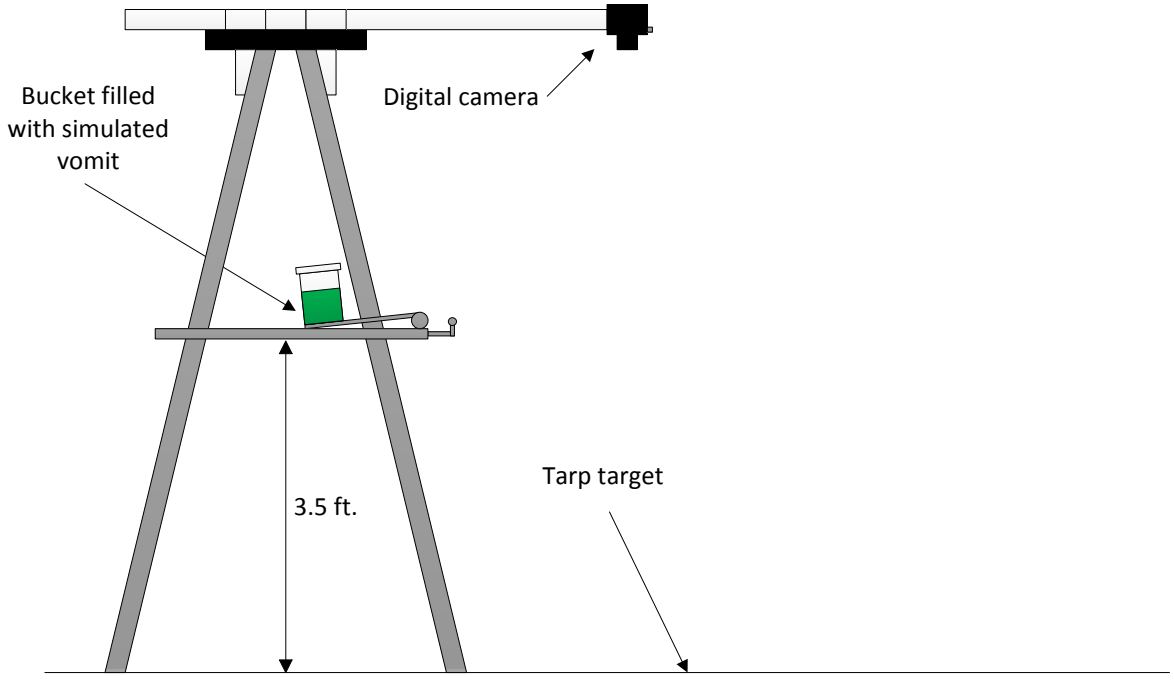

Figure 11. Tipping Bucket Experimental set-up

Experimentation with Simulated Vomitus

Volumes used in the experiment included: 50, 100, 200, 300, 400, 500, 600, 700, and 800 ml. According to the expert consultation, volumes higher than 800 ml would not be typical during vomiting (Kenneth Koch, 2011). A minimum volume of 50 ml was chosen under the assumption that a lower volume would not produce a significant amount of splatter. Each volume was tipped from the bucket onto the tarp five times. To tip the bucket, the experimenter used one hand to lift the bucket until the tipping point at which time the bucket fell freely until hitting the break bar. A break bar was used to stop the bucket and propel the vomitus on the tarp, shown in Figure 12. During each tip the experimenter did his/her best to aim the vomitus for the "+" marked on the tarp to keep the splatter centered. Using a remote control, the experimenter captured an orthogonal digital image for each oatmeal trial. Digital images for the artificial saliva trials were not captured because the splatter images were outside the range of the camera's focus. The digital image was uploaded into ImageJ, an image analysis program (http://rsbweb.nih.gov/ij/). Oatmeal images were scaled using the visible black rings on the tarp target. Slight adjustments were made to the images' contrast and color to create a clear definition between the vomitus splatter and background. The oatmeal images were then converted to binary images to clearly show the splatter pattern; the vomitus splatter was shown as black and the background as white. A function in the ImageJ program measured the spatial area covered by the black image (vomitus). Using a measuring tool in the program, the distance from the center of vomitus splatter to the furthest droplet was recorded. Since the saliva trials created splatter areas that were too big to be captured by

the camera, the furthest distance traveled by droplets was measured using a tape measure. Visual judgment was used to locate the center of splatter for oatmeal and saliva trials.

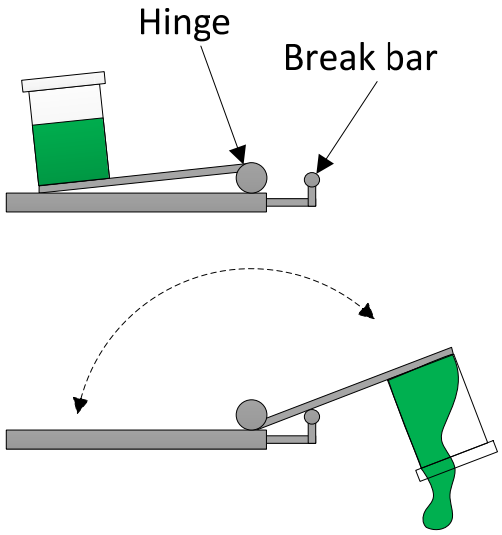

Figure 12. Break bar

Results and Discussion

The average dynamic viscosities of the oatmeal and simulated saliva matrix were 3499 mPa*s and 1.55 mPa*s, respectively. Artificial saliva has a dynamic viscosity very similar to water which is 1 mPa*s at 20°C. Binary images processed by the ImageJ software for the five oatmeal trials are shown in Figure 14through Figure 18; the figures are not shown to scale. Splatter surface areas typical of each oatmeal volume are shown in Figure 19. Distances measured from the center of vomitus splatter to the furthest droplet are shown in Figure 20 and Figure 21. Oatmeal has a higher viscosity than artificial saliva and therefore

did not splatter as far when tipped; this means when using oatmeal a larger volume of the vomitus remained closer to the initial impact spot compared to artificial saliva. Splatter patterns in Figure 14 through Figure 18 show that oatmeal trials produced droplets that were more globular than artificial saliva. Artificial saliva was more watery than oatmeal and produced spray patterns rather than the globular droplet patterns observed for the oatmeal trials; an example of an artificial saliva spray pattern is on the tarp target shown in Figure 13.

Figure 13. Example of artificial saliva splatter pattern (Trial 5, 600ml)

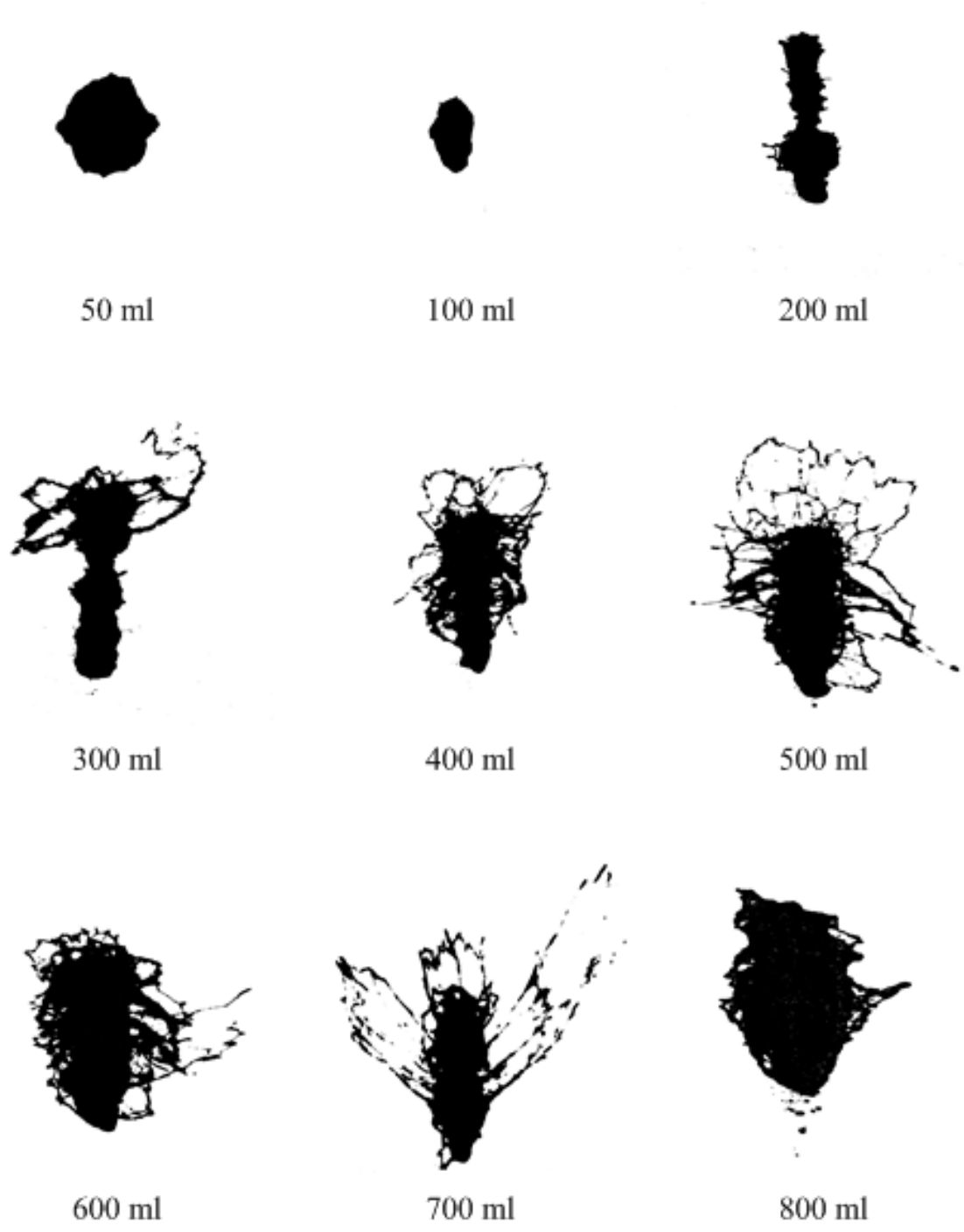

Figure 14. Oatmeal Trial 1

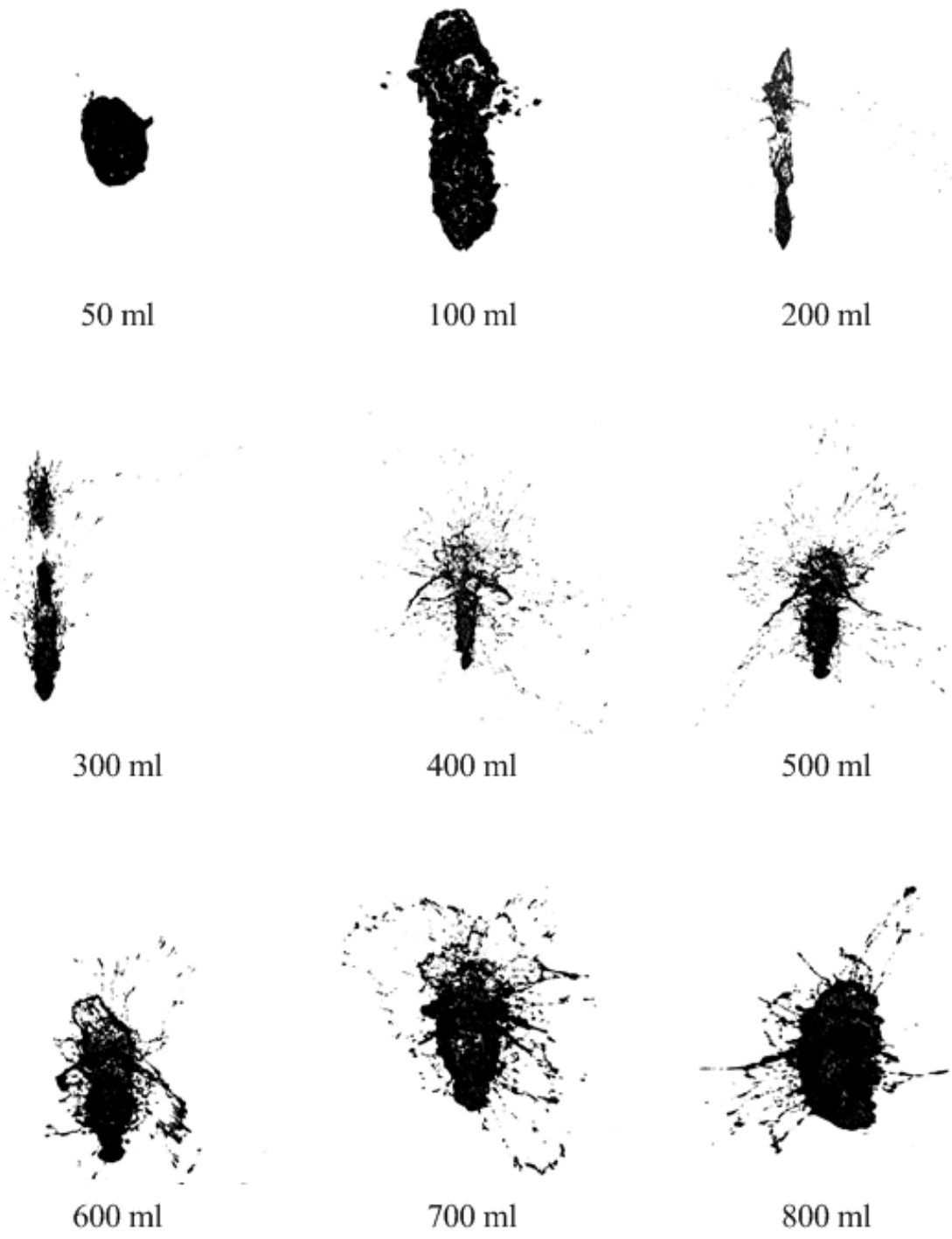

Figure 15. Oatmeal Trial 2

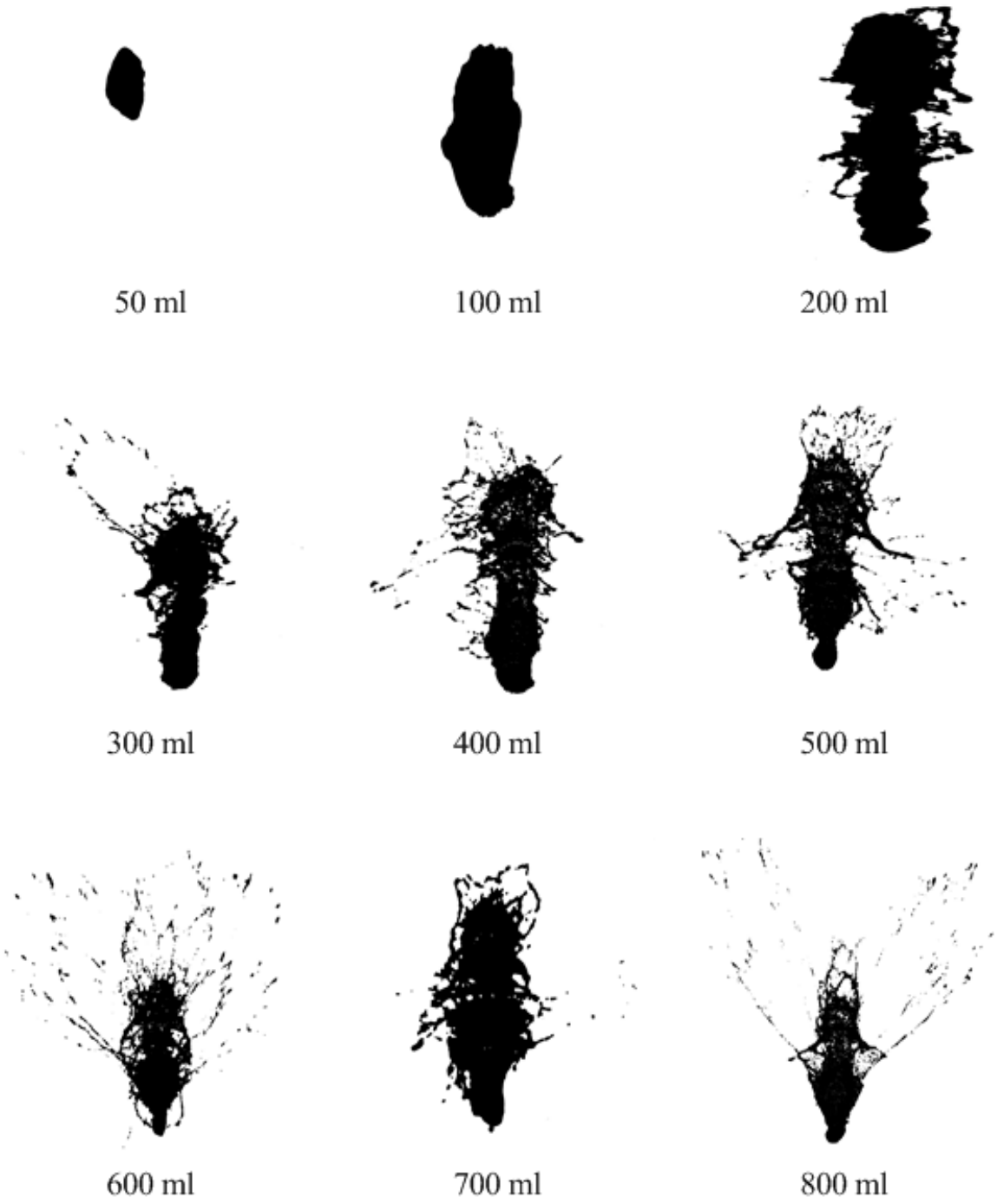

Figure 16. Oatmeal Trial 3

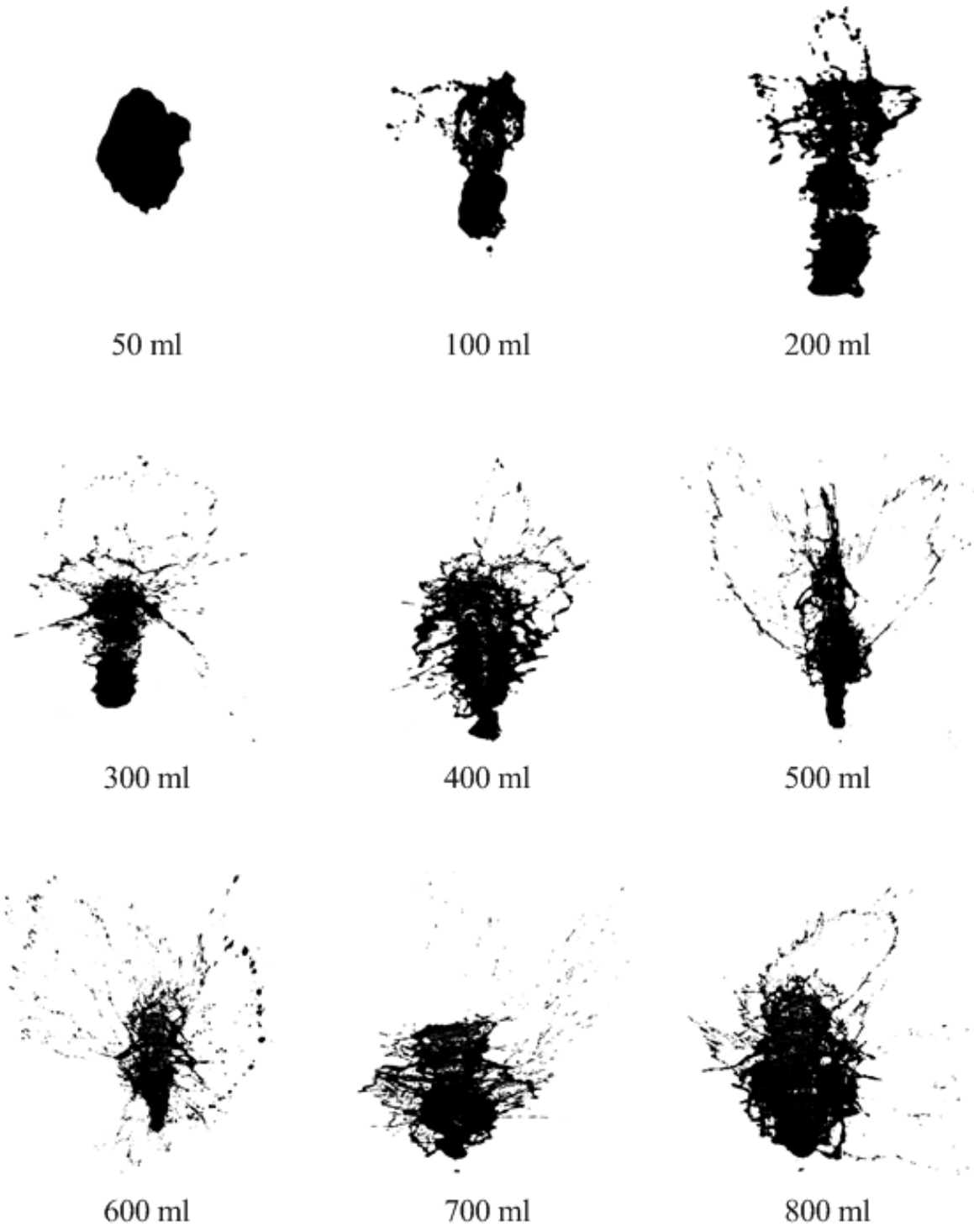

Figure 17. Oatmeal Trial 4

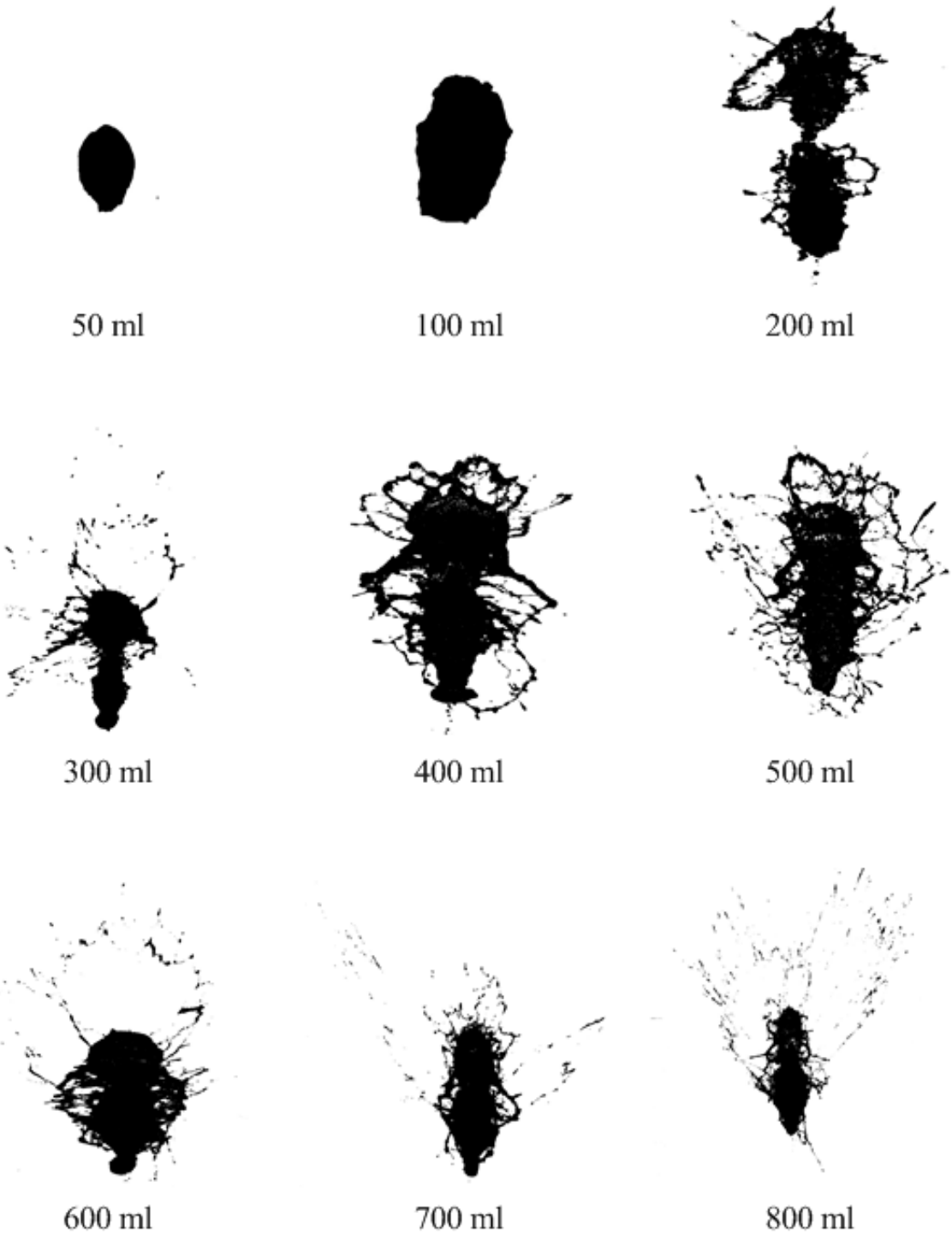

Figure 18. Oatmeal Trial 5

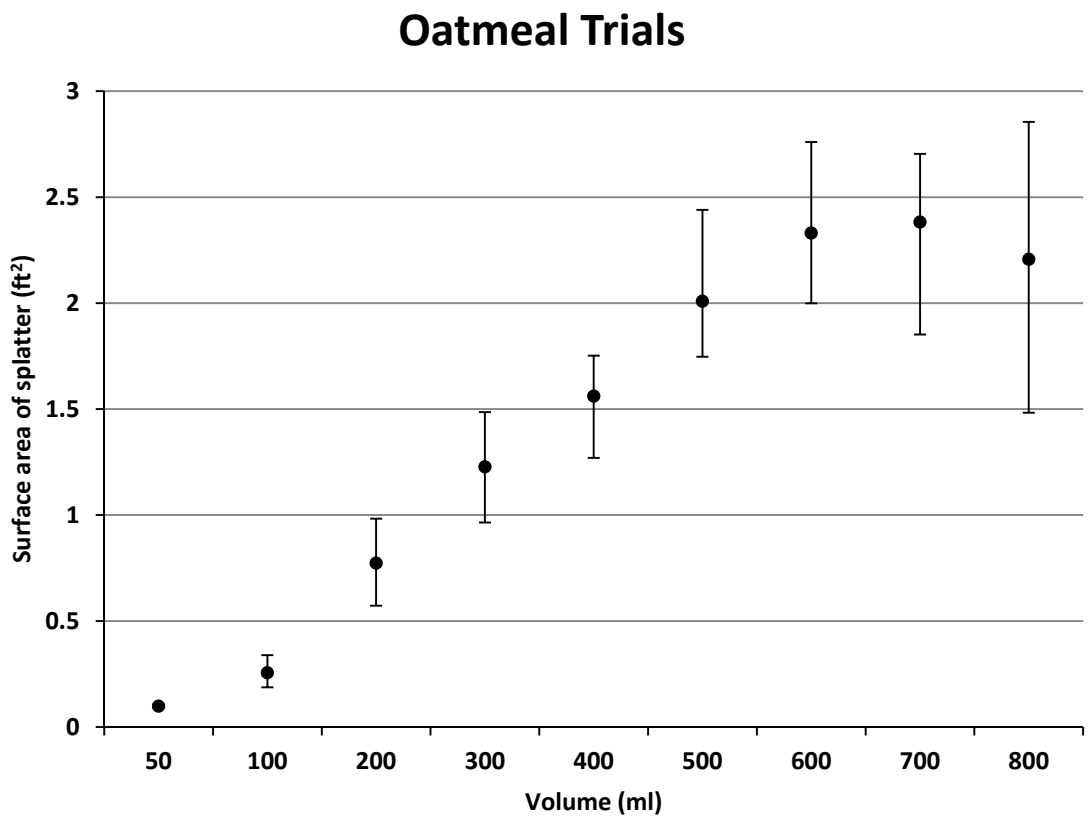

Figure 19. Surface area covered by oatmeal splatter (average values appear as dots and error bars represent minimum and maximum values)

The average surface area of oatmeal splatter increases with the volume of oatmeal used until a volume of 600 ml. Volumes greater than 600 ml did not show a significant increase in average splatter surface area as seen in Figure 19. For the oatmeal trials, the distance of the furthest droplet from the center of splatter was 4.625 ft. This distance was 14.5 ft. for the saliva studies.

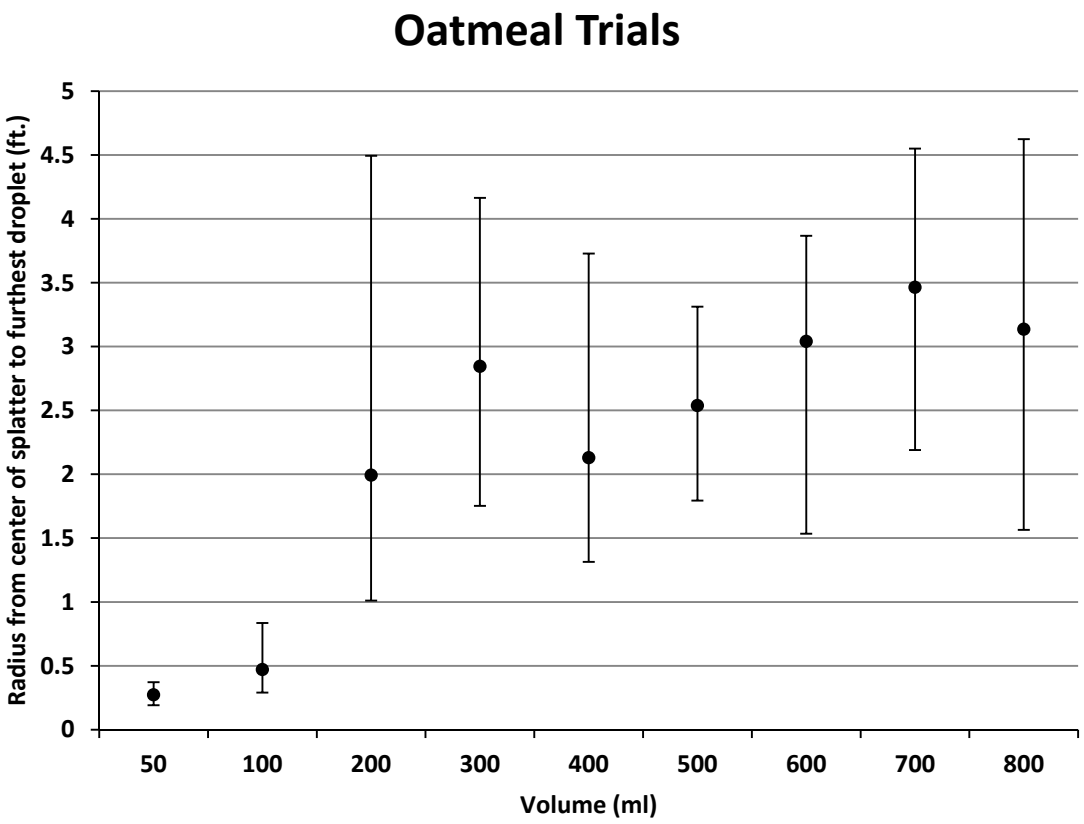

Figure 20. Furthest distances traveled by droplets in oatmeal trials

The furthest distance traveled by an oatmeal droplet was highly dependent upon volume, with the mean distance traveled ranging from 3-3.5 ft. for higher volumes (≥600 ml) as shown in Figure 20. On the other hand, regardless of volume, artificial saliva experiments yielded a mean distance of 8-12 ft.; the greatest distance traveled in any one experiment was 14.5 ft. as shown in Figure 21.

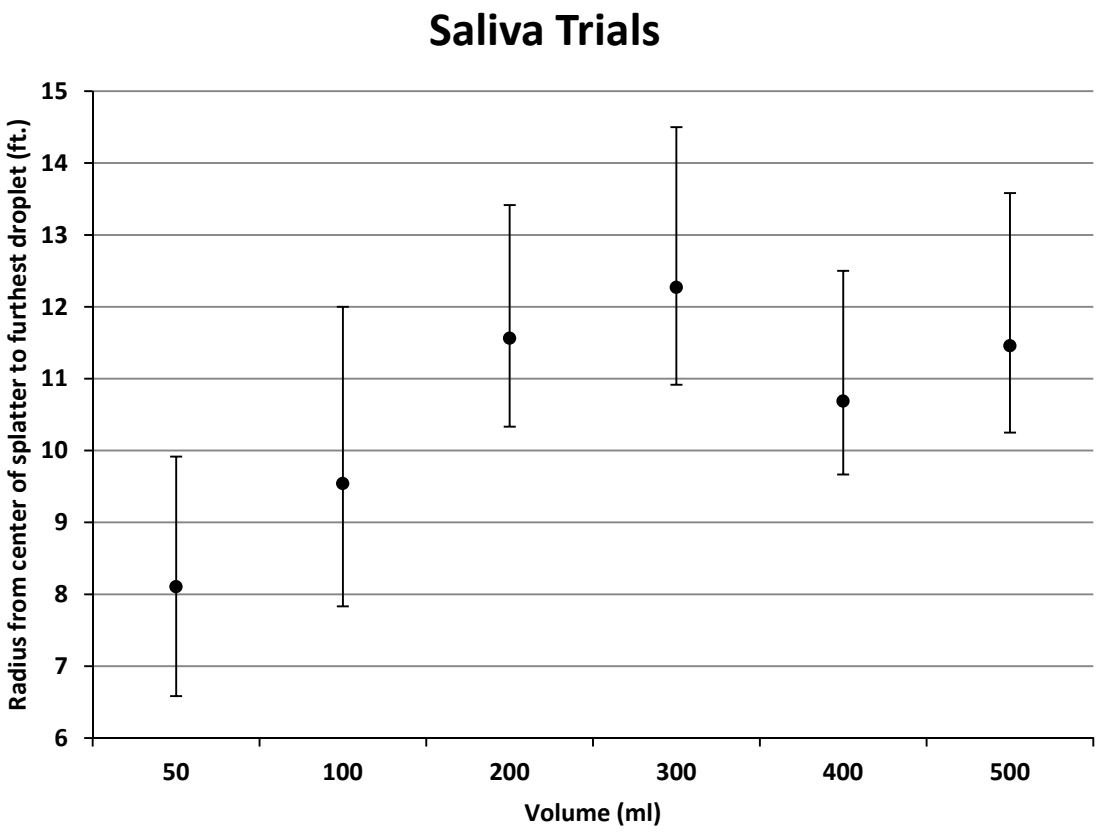

Figure 21. Furthest distances traveled by droplets during saliva trials

Conclusions

These measurements suggest that vomitus splatter can be deposited up to 15 ft. away from the initial vomiting impact location, which provides some guidance as to the area that may need to be cleaned and decontaminated after a primary vomiting event. The technique used in the methodology to locate the center of the vomitus would be similar to the technique used by facility personnel. Although the experimental design for this study is somewhat crude, we can suggest that a circular zone with a diameter of up to 30 feet might be a

cautious estimate for a clean-up area. In the future, results from clinical vomiting studies using human patients to examine the splatter of vomitus can be done to compliment this experiment.

The Tipping Bucket experiment used a flat, level surface for splattering vomitus; this made measuring splattering distances easier than if a complex surface with many edges and surface angles was used. However, in a realistic vomiting scenario, vomitus could splatter onto many different surfaces including: tables, chairs, walls, water fountains, etc., during a vomiting episode. Vomiting on complex surfaces could produce different splatter patterns (e.g. splatter ricochet) than the ones observed in the Tipping Bucket experiment and could potentially change the recommended clean-up zone; this type of vomiting scenario merits further research.

CHAPTER 4: DEVELOPING A VOMITING MACHINE MODEL

Introduction

Epidemiological studies examining the transmission of HuNoV during outbreaks suggest that that viruses can become airborne during vomiting and potentially expose nearby persons (Ho et al., 1989)(Weinstein, Said, Perl, & Sears, 2008)(Morawska, 2006). The importance of studying the aerosolization of NoV during vomiting is crucial to any high occupancy facility cleaning plans because airborne NoV could potentially extend the zone of contamination far beyond the range of vomitus splatter. The goal of this study was to create a laboratory model that can simulate a vomiting episode that is physically similar to a human vomiting episode. A human full-scale model would require an infrastructure too big to maintain in a sterile lab environment, thus a scaled version of the model was produced. To simulate a vomiting episode similar to a human, a scaled vomiting model must include components that mimic a mouth, an esophagus, and a stomach. A small containment chamber was used to house the scaled vomiting model and protect the lab environment from any material used during a vomiting episode simulation. This chapter describes the methods and materials used to construct a vomiting machine model.

Methods and Materials

Similitude Overview

Similitude is a concept in fluid mechanics that is used to make a scaled engineering model similar to a full-scale prototype. In this project the full- scale prototype is defined as

the human upper gastrointestinal tract complete with mouth, esophagus, and stomach; in this chapter, the human prototype will be referred to as the "human body" and/or have an "h" subscript. This project used similitude to produce a scaled engineering model that behaves similarly to a full-scale human upper gastrointestinal tract. Achieving similitude in an engineering model is based on three types of similarity to the full-scale application: geometric, kinematic, and dynamic (Fox Robert, McDonald Alan, & Pritchard Philip, 2004). Having geometric similarity in an engineering model means that the model and prototype must have the same shape and that all of the linear dimensions of the model must be related to corresponding dimensions in the prototype by the same scaling factor (Fox Robert et al., 2004). A requirement for kinematic similarity is that velocities at corresponding points in the model and prototype must have the same direction and differ by the same constant scale factor (Fox Robert et al., 2004). Dynamic similarity means that the ratios of all the forces acting on the fluid particles are constant between the engineering model and the prototype. To achieve dynamic similarity certain dimensionless groups such as the Reynolds Number and Euler's Number must have the same value in the model and the prototype. The Buckingham Pi theorem is a procedure to identify the dimensionless groups, also known as π groups, appropriate for a given fluid mechanics problem. The goal of this project was to produce a scaled model that will have fluid flow through a surrogate esophagus that is similar to vomitus flow during a projectile vomiting episode in a human prototype.

Determining π Groups

The first step in determining the π groups is to list all the dimensional parameters that affect the fluid flow in the fluid mechanics problem; the number of dimensional parameters in this list is denoted by the term n. Flow through the human esophagus and surrogate esophagus will be treated as flow through a smooth pipe. Dimensional parameters that affect fluid flow through a smooth pipe are: Δp (pressure change), D(pipe diameter), V (fluid velocity), ρ (fluid density), and μ (fluid dynamic viscosity); thus n = 5 (Munson & Okiishi, 2002). Figure 22 shows the flow of a cross section of fluid through both the prototype and model; dimensional parameters are shown respectively.

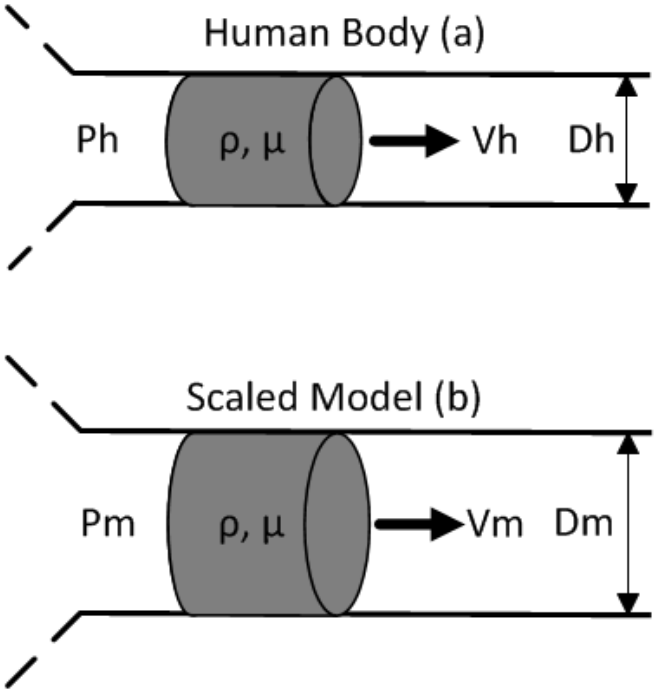

Figure 22. Diagram of fluid flow in (a) human body and (b) scaled model

The second step is to list all of the primary dimensions that are found in the dimensional parameters; the number of primary dimensions is noted by the term *m.* The primary dimensions found in the dimensional parameters include: M (mass), L (length), and T (time); thus $m = 3$. The following dimensional parameters are listed in the form of their primary dimensions: $\Delta p \left(\frac{M}{T^2 L}\right), D(L), V \left(\frac{L}{T}\right), \rho \left(\frac{M}{L^3}\right), \mu \left(\frac{M}{LT}\right)$.

The third step is to select a group of repeating dimensional parameters that will appear in all of the π groups. One requirement for a repeating dimensional parameter is that it cannot have dimensions that are a power of another dimensional parameter. For instance, in this situation Δp and μ cannot be repeating dimensional parameters because they have dimensions $(MT^{-2}L^{-1})$ and $(MT^{-1}L^{-1})$, respectively. Next, the Buckingham's π theorem is used to determine the number of dimensionless groups needed for dynamic similarity. The theorem states that *n-m* dimensionless groups are needed; thus two π groups are needed for this fluid mechanics problem.

The first π group should follow the functional form show in Equation(4.1), and includes all of the repeating dimensional parameters and Δp, one of the two non-repeating dimensional parameters. For the 1st π group to be dimensionless, Equation (4.2) must hold true for the values of the exponents: $a, b, and\ c$.

$$\pi_1 = \Delta p \cdot D^a \cdot V^b \cdot \rho^c \tag{4.1}$$

$$\pi_1 = \left(\frac{\mathrm{M}}{\mathrm{T^2 L}}\right) \cdot (\mathrm{L})^{\mathrm{a}} \cdot \left(\frac{\mathrm{L}}{\mathrm{T}}\right)^{\mathrm{b}} \cdot \left(\frac{\mathrm{M}}{\mathrm{L^3}}\right)^{\mathrm{c}} = \mathrm{M}^0 \cdot \mathrm{L}^0 \cdot \mathrm{T}^0 \tag{4.2}$$

$$M\ balance: 1 + c = 0 \tag{4.3}$$

$$T\ balance: -2 - b = 0 \tag{4.4}$$

$$L\ balance: -1 + a + b - 3c = 0 \tag{4.5}$$

To solve for the exponents of the dimensional parameters in Equation (4.2), each dimension is balanced on both sides of the equation as shown in Equations (4.3), (4.4) and (4.5). Solving the equations simultaneously yields the following values: $c = -1, b = -2, a = 0$. Substituting the exponents into Equation (4.1) yields the 1st π group, shown in Equation (4.6).

$$\pi_1 = \frac{\Delta p}{V^2 \cdot \rho} \tag{4.6}$$

The 2nd π group includes all of the repeating dimensional parameters and μ, the second of the two non-repeating dimensional parameters, seen in Equation (4.7). For the 2nd π group to be dimensionless, Equation (4.8) must hold true for the values of $d, e, and\ f$.

$$\pi_2 = \mu \cdot D^d \cdot V^e \cdot \rho^f \tag{4.7}$$

$$\pi_2 = \left(\frac{M}{L \cdot T}\right) \cdot (L)^d \cdot \left(\frac{L}{T}\right)^e \cdot \left(\frac{M}{L^3}\right)^f = M^0 \cdot L^0 \cdot T^0 \tag{4.8}$$

$$M\ balance: 1 + d = 0 \tag{4.9}$$

$$T\ \ balance: -1 - e = 0 \tag{4.10}$$

$$L\ balance: -1 + d + e - 3f = 0 \tag{4.11}$$

To solve for the exponents of the dimensional parameters in Equation (4.8), each dimension is balanced on both sides of the equation as shown in Equations (4.9), (4.10) and

(4.11). Solving the equations simultaneously yields the following values: $d = -1, e = -1, f = -1$. Substituting the exponents into Equation (4.7) yields the 2nd π group, shown in Equation (4.12).

$$\pi_2 = \frac{\mu}{D \cdot V \cdot \rho} \tag{4.12}$$

Recall that dynamic similarity is achieved when the π groups have the same value in the model and in the prototype. Note that the 1st π group is closely related to a common dimensionless parameter used in fluid mechanics, known as the Euler number or pressure coefficient. The relationship between the 1st π group and the pressure coefficient is shown in Equation (4.13). Additionally, the 2nd π group is similar to a common dimensionless parameter known as the Reynolds number; its relationship is shown in Equation (4.14) (Fox Robert et al., 2004).

$$\pi_1 = \frac{1}{2} \cdot (C_p) \tag{4.13}$$

$$\pi_2 = (\mathrm{Re})^{-1} \tag{4.14}$$

Since the Reynolds number and pressure coefficient are common dimensionless parameters and are easy to work with mathematically, they will be used as the dimensionless groups to achieve dynamic similarity in the scaled model (Fox Robert et al., 2004). Equations (4.15) and (4.16) show that the Reynolds number and pressure coefficient must be the same for both the scaled model (denoted by the *m* subscript) and the human body (denoted by the *h* subscript).

$$Re_h = Re_m = \left(\frac{\rho_h D_h V_h}{\mu_h} \right) = \left(\frac{\rho_m D_m V_m}{\mu_m} \right) \tag{4.15}$$

$$Cp_h = Cp_m = \left(\frac{\Delta p_h}{\frac{1}{2}\rho_h V_h^2} \right) = \left(\frac{\Delta p_m}{\frac{1}{2}\rho_m V_m^2} \right) \tag{4.16}$$

Achieving Similitude

Using the dimensions of the human parameters, outlined in Chapter 1, several trial-and-error scales where used to determine which scale would create the easiest assembly with respect to material availability. Approximately a four to one scale was used to construct the vomiting machine device. Geometric similarity was achieved by scaling every linear dimension down in the model; Equation (4.17) shows the scale between the diameter of the human esophagus and the diameter of the model surrogate esophagus, denoted by D.

$$Scale = \frac{D_h}{D_m} = \frac{9.84\ in}{2.5\ in} = 3.94 \tag{4.17}$$

Shown in Table 3 are the values of all the scaled linear dimensions in the model using the scale from Equation (4.17). In some cases, the dimension of the scaled parameter was rounded to the nearest available dimension offered by product manufacturers, as shown in Table 3.

Table 3. Machine Model Parameter Dimensions

Scaled Machine Dimensions		
	(in)	(cm)
Esophagus Length	2.5	6.35
Esophagus Diameter	0.25	0.635
Mouth Length	1	2.54
Mouth Diameter	0.5	1.27

Surrogate vomitus used inside the scaled model will be a solution of 0.5% carboxymethylcellulose (CMC) which has a viscosity of 500 mPa*s. For similitude purposes, an assumption will be made that the vomitus fluid inside the scaled model is the same as vomitus inside the human body. Assuming that the fluid is the same in the model as it is in the prototype, Equation (4.15) reduces to Equation (4.18).

$$\left(D_h V_h\right) = \left(D_m V_m\right) \tag{4.18}$$

Rearranging Equation (4.18) and substituting Equation (4.17) reveals the constant scale factor for velocities shown in Equation (4.19).

$$\frac{V_h}{V_m} = \frac{D_m}{D_h} = \frac{1}{3.94} \tag{4.19}$$

Velocities of vomitus inside the human body and the scaled model are unknown at this time. Since the specific velocity values in the model and the human body are unknown, Equation (4.19) will serve primarily as a guide to the ratio of velocities rather than to the specific values of velocities.

The governing dimensional parameter of our scaled model will be pressure. Recall from Chapter 1 that pressure build up in the stomach is the main driving force that causes projectile vomiting. The pressure coefficient will be more of concern than Reynolds number when proving dynamic similarity because the pressure coefficient has a pressure term in its dimensionless group. Under the assumption that the same fluid is used in the model as in the prototype, Equation (4.16) reduces to Equation (4.20). Rearranging Equation (4.20) and solving for Δp_m, change in pressure in the model, yields Equation (4.21).

$$\frac{\Delta p_h}{V_h^2} = \frac{\Delta p_m}{V_m^2} \tag{4.20}$$

$$\Delta p_m = \Delta p_h \cdot \left(\frac{V_m}{V_h} \right)^2 \tag{4.21}$$

Combining the reduced Reynolds number expression, Equation (4.19), into Equation (4.21) reveals Equation (4.22).

$$\Delta p_m = \Delta p_h \cdot (3.94)^2 \tag{4.22}$$

The change in pressure term, Δp is defined as the difference in local pressure, p minus the freestream pressure, p_∞ as shown in Equation (4.23) (Fox Robert et al., 2004). In both the model and the prototype, the freestream pressure is zero. The local pressure, p_p, in the prototype will be at the point where the esophagus connects to the stomach and the local pressure in the model, p_m, will be at the point where the surrogate esophagus connects to the stomach chamber.

$$\Delta p = p - p_{\infty} \tag{4.23}$$

Since the freestream pressures are zero, Equation (4.22) reduces to Equation (4.24).

$$p_m = p_h \cdot (3.94)^2 = p_h \cdot 15.5 \tag{4.24}$$

Model Construction

According to the expert consultation, conserving the shape of the human stomach is not necessary in the design of the stomach chamber in the machine (Kenneth Koch, 2011). A clear PVC tube three inches long was chosen as the stomach chamber so the experimenter could observe the reactions inside in the chamber. At either end of the PVC tube, a gray PVC cap was screwed on to either end to seal the chamber. A brass check valve was screwed into the center of one of the gray PVC caps; this is the chamber bottom. The reason for using a check valve is to keep air from escaping when pressurizing the chamber. Screwed to the check valve is a brass ¼" barb, this barb connects the ¼" Tygon tubing from the stomach chamber to a hand operated air pump. At the other end of the stomach chamber, a brass ball valve is screwed into the center of the PVC cap at the top of the chamber. The ball valve represents the lower esophageal sphincter (LES); in a human body this is the organ that releases vomitus from the stomach. Another ¼" brass barb connects to the other end of the ball valve. Tygon tubing 2.5 inches long is attached to the brass barb acting as a surrogate esophagus. Connected to the end of the esophagus is an expansion fitting that leads into a 1 inch length of ½ inch diameter tubing which mimics the human mouth. In this study, the human mouth is treated as a circular length of tubing; the human tongue and teeth are not

included in the model design. A psi gauge is attached to the top end of the PVC cap; this gauge reads the pressure at the connection between the surrogate esophagus and the stomach chamber. Using the pump and pressure gauge, the stomach is pressurized to one of the scaled pressures listed in Table 6. After the stomach chamber is pressurized and the ball valve is opened, a wooden piston 1" in diameter inside the stomach chamber acts as a piston and helps push the vomitus out of the stomach into the esophagus. Vomitus travels through the esophagus in a slight curve to simulate the extension of the neck during a vomiting episode. A makeshift clay mold of the human face is attached to the mouth; this is mainly for aesthetic reasons. The model design is shown in Figure 17.

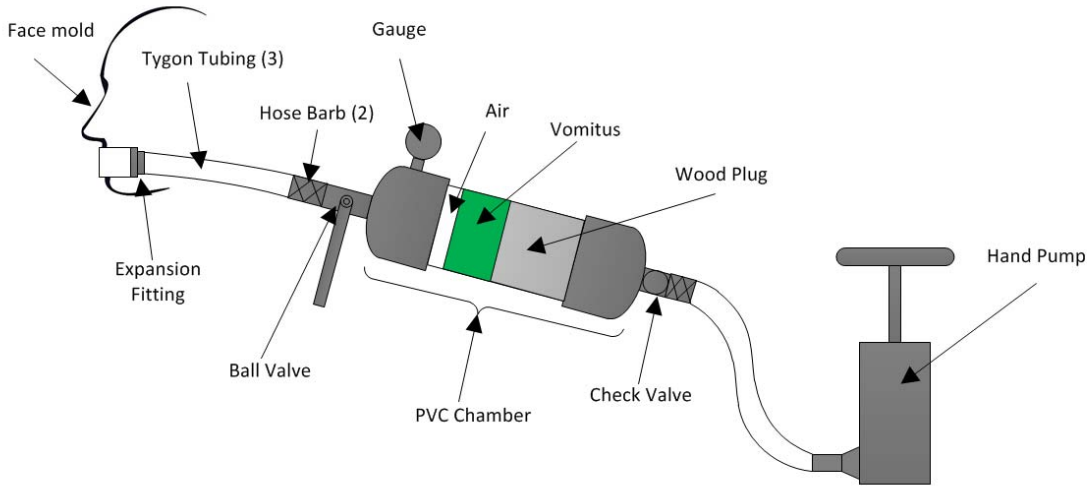

Figure 23. Diagram of vomiting device model

Vomitus, Piston, and Pressure Scaling

The design of the stomach chamber allows different volumes of surrogate vomitus to be used when simulating vomiting episodes. Table 4 lists four typical volumes of vomitus, volumes of air, and total stomach volumes that could be observed during a vomiting episode in the human body. Volume is a cubic dimension so the linear scale factor from Equation (4.17) must be cubed when scaling; Table 5 shows the scaled surrogate vomitus volume, air volume and total stomach chamber volume.

Pressures observed in the human stomach are scaled to the pressures used in the model stomach chamber using Equation (4.24). Table 6 shows a summary of the maximum, average, and minimum pressures observable in the human stomach with corresponding scaled pressures for the stomach chamber.

Table 4. Typical volumes of vomitus and air that could be observed during a vomiting episode

Human Body		
Vomitus Volume (ml)	Air Volume (ml)	Total Stomach Volume (ml)
800	200	1000
600	200	800
400	200	600
200	200	400

Table 5. Scaled down volume sizes for the vomiting machine model

Surrogate Vomitus Volume (ml)	Scaled Model Air Volume (ml)	Total Chamber Volume (ml)
12.5	3.1	15.6
9.4	3.1	12.5
6.25	3.1	9.35
3.1	3.1	6.2

Table 6. Scaled stomach chamber pressures

	Human Stomach (psi)	Stomach Chamber (psi)
Maximum	5.6	86.8
Average	1.6	24.8
Minimum	0.77	11.9

Including a wooden piston inside the stomach chamber serves two purposes: (1) It can easily be exchanged for a different size to accommodate the change in desired surrogate vomitus; and (2) It acts as a piston and helps push out surrogate vomitus when simulating a vomiting episode. When empty, the stomach chamber is 1" in diameter and 3.9" in length. To calculate the required piston size for a specific stomach chamber volume, the volume must first be converted into a length assuming 1" diameter and then subtracted from the chamber's total length, 3.9". Equation (4.25) illustrates how to convert a stomach chamber volume into a length assuming 1" diameter.

Table 7 lists the lengths of piston corresponding to the total stomach chamber volumes.

$$Plug\ Length\ (in) = 3.9 - \left(\left(\frac{TotalChamberVolume\ (ml)}{16.387} \right) \cdot \left(\frac{1}{\pi \cdot \left(\frac{1"diameter}{2} \right)^2} \right) \right) \quad (4.25)$$

Table 7. Piston lengths corresponding to the total chamber volumes

Scaled Model	
Total Chamber Volume (ml)	Piston Length (in)
15.6	2.47
12.5	2.75
9.35	3.04
6.2	3.33

Containment Chamber Design

A containment chamber was constructed from plexiglass wall panels with a hinged lid. The dimensions are 12”x12”x 17.5” which holds 61.7 liters of air; all corners and edges were sealed with silicone and the lid was sealed with weather proofing tape, as shown in Figure 18. During experimentation, a heavy object is recommended to be placed on top of the lid to keep a tight seal. To quantify bioaerosols in later experimentation, a SKC Biosampler© will be used to collect any bioaerosols present inside the air chamber. Four milliliters of phosphate buffers solution (PBS++) will be used as the collection liquid in the collection vessel of the Biosampler (Fabian, McDevitt, Houseman, & Milton, 2009). The Biosampler has three tangential nozzles in the collection vessel, as shown in Figure 25, which act as sonic orifices. According to the manufacturer of the biosampler, if the downstream vacuum pressure remains at 15 Hg, the sonic orifices maintain the collection rate

at 12.5 L/min (SKC, 2012). The Biosampler is connected to the center side of the air chamber by a piece of Tygon tubing and a hose barb; this is known as the Biosampler port. A water trap is connected downstream of the Biosampler by a piece of Tygon tubing to prevent fluid traveling into the vacuum pump. To prevent any bioaerosols from leaving the air chamber system, a HEPA filter is placed in parallel with the water trap. Finally, a vacuum pump and gauge control the suction to the Biosampler. Inside the air chamber is a Thermo-Hygro sensor that displays instantaneous temperature and relative humidity.

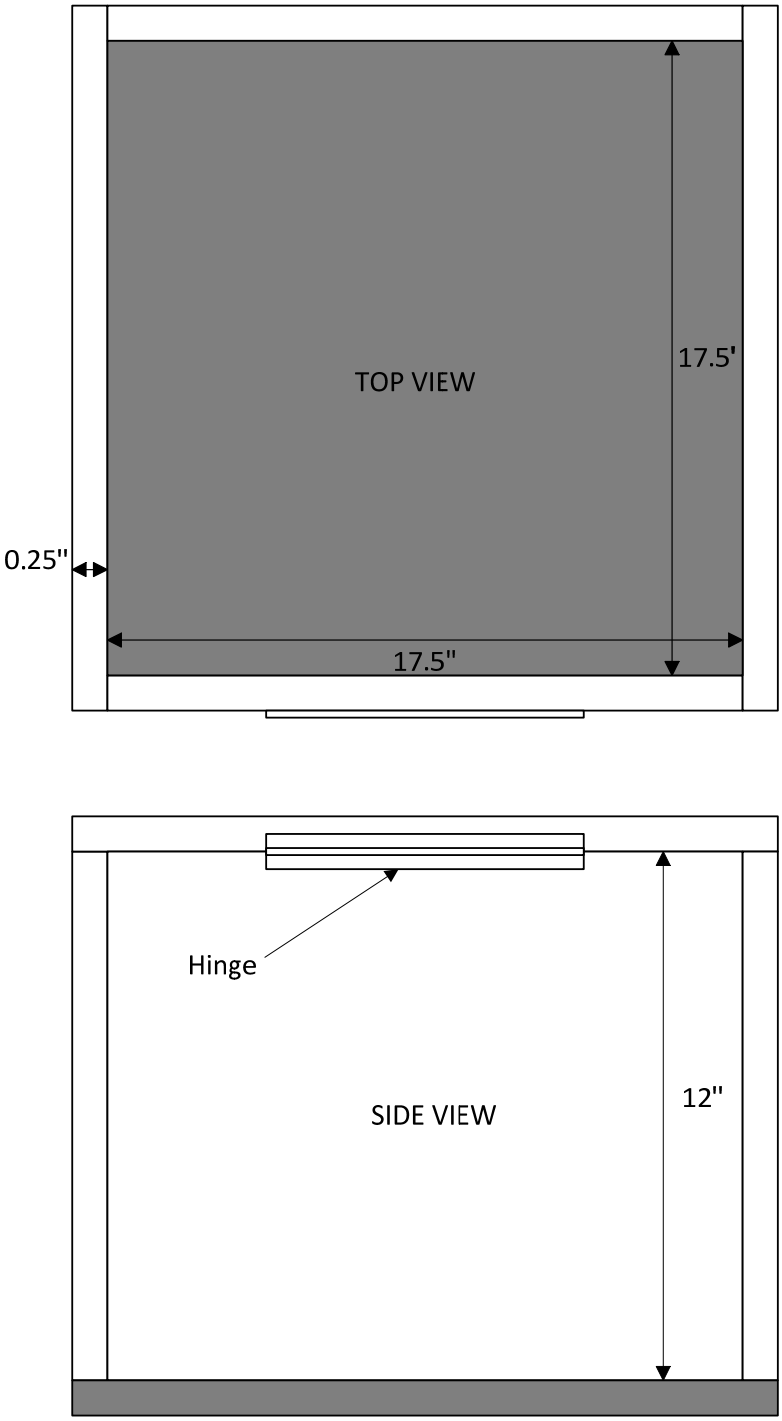

Figure 24. Air chamber dimensions

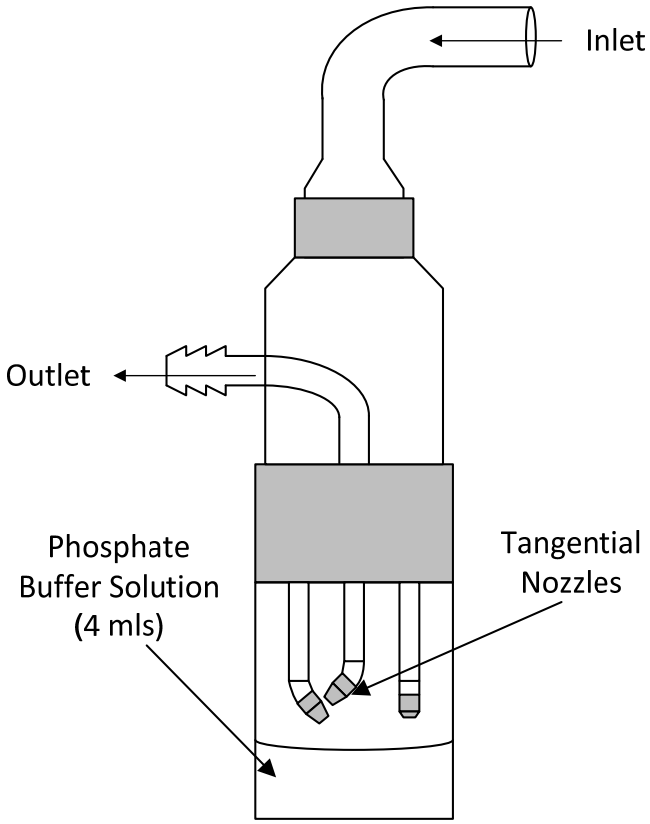

Figure 25. Diagram of the SKC Biosampler

The vomiting machine is connected to the air chamber using a rubber stopper with the center removed so the surrogate esophagus can pass through. The majority of the model remains outside the air chamber supported by a metal lab stand. Inside the chamber, the clay face mold and mouth point at a slight angle towards the ground. When future experiments are conducted, the goal is for the Biosampler to collect only bioaerosols and not any splatter material. The slight angle will prevent any splatter from landing inside the Biosampler port.

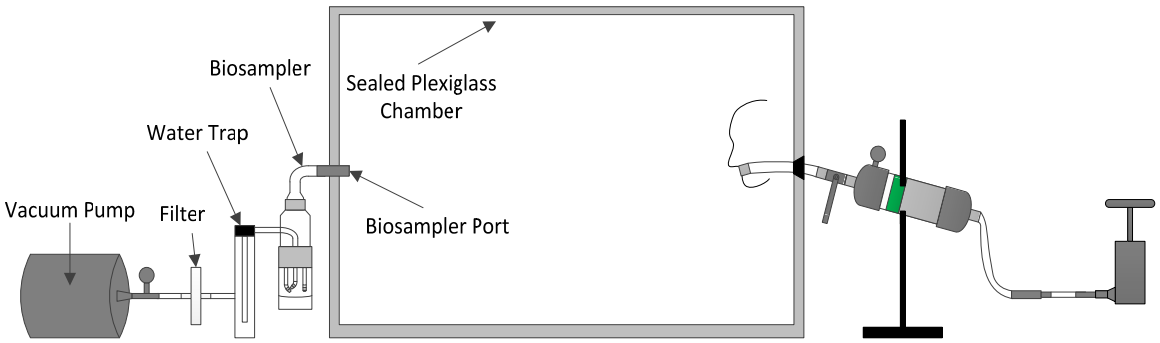

Figure 26. Vomiting device housed inside air chamber

Results and Discussion

Figure 27 shows the fully constructed vomiting machine attached to air chamber. The position of the clay face mold and the model mouth are slightly aimed towards the bottom of the air chamber.

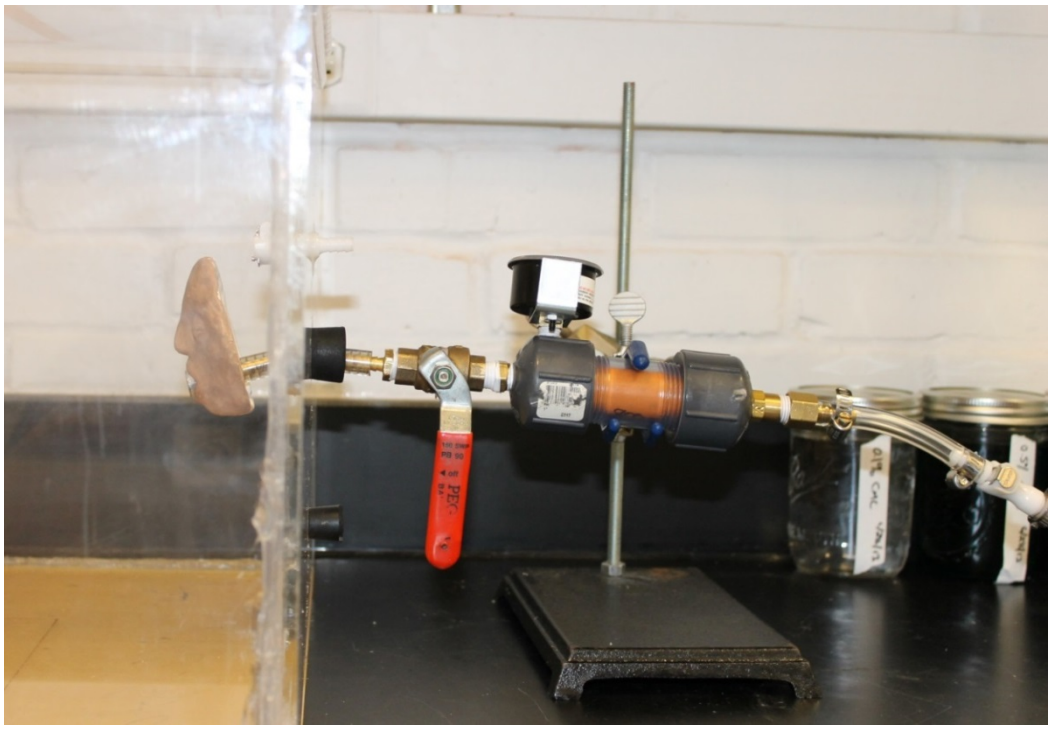

Figure 27. Picture of the vomiting device attached to the air chamber

Figure 28 shows a picture of surrogate vomitus leaving the model mouth during the middle of a simulation of a vomiting episode. The surrogate vomitus volume used was 12.5 ml and the amount of air in the chamber was about 3 ml; these volumes correspond to a human vomitus volume of 800 ml and an air volume of 200 ml. The stomach chamber was pressurized to 24.8 psi before the brass ball valve was pulled, which released the surrogate vomitus.

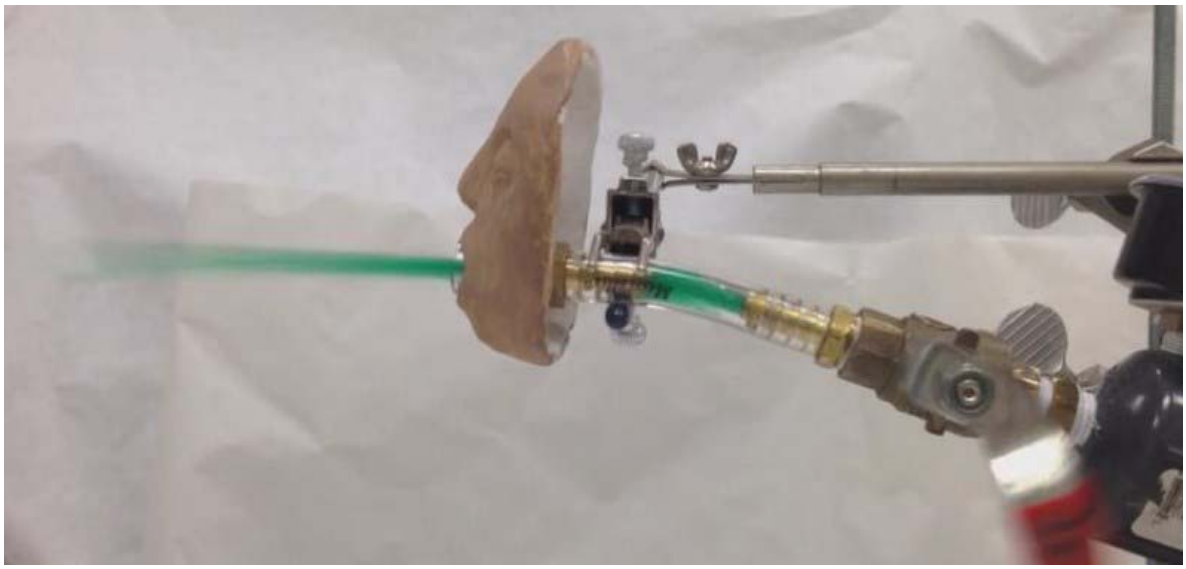

Figure 28. Picture of the vomiting machine simulating a vomiting episode right as the surrogate vomitus exits the mouth

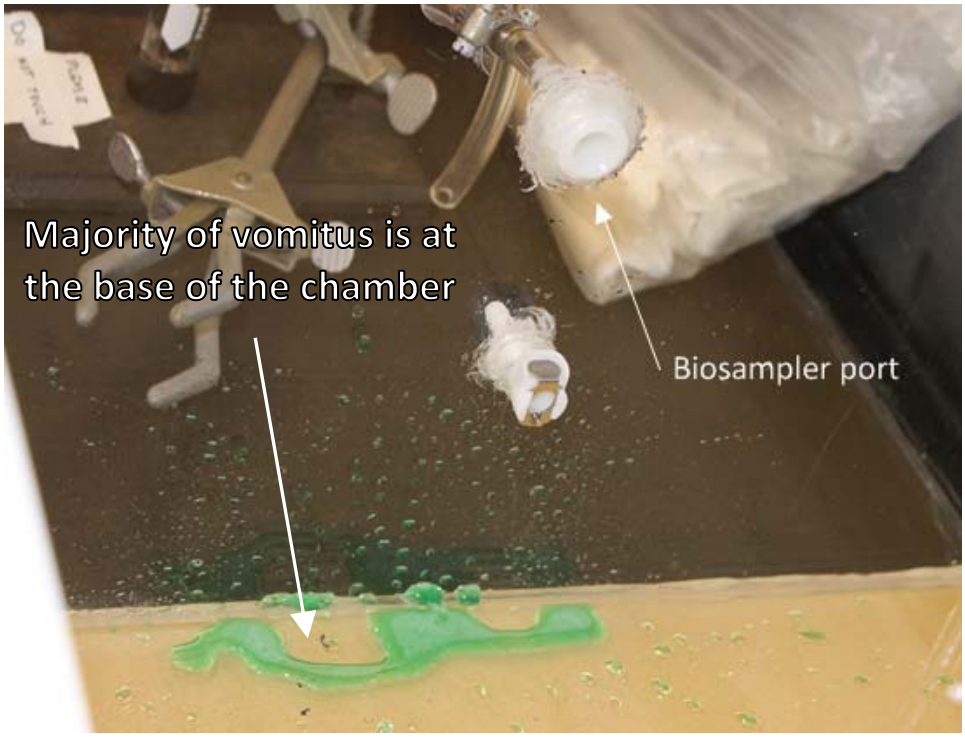

Figure 29. Picture of the inside of the air chamber after a simulation of vomiting

After a vomiting episode simulation, the surrogate vomitus lands at the bottom of the air chamber and around the edges of the sides. Figure 29 shows that surrogate vomitus does not hit the Biosampler port during a simulation; this is desired so that during later experimentation there will not be any interference with bioaerosol collection.

Using the Containment Chamber and Biosampler

Although the Biosampler has a very high rated collection efficiency, nearly 100% over a wide range of particle sizes, certain experimental factors such as chamber geometry, equipment orientation, and sampling periods could cause lower Biosampler efficiencies (SKC, 2012). It is important to test the collection efficiency of the containment system before experimentation. A collision nebulizer can be used to introduce a known amount of aerosolized particles into the containment chamber. After a sampling period, the amount of particles in the Biosampler collection vessel can be measured. Efficiency of the system is defined as the ratio between the amount of particles introduced and the amount of particles captured by the Biosampler. Some of the particles introduced into the containment chamber by the nebulizer are small enough that they are able to remain airborne for long periods of time. At short sampling times there is a good chance that small particles may not have come into contact with the streamline of the Biosampler and they could still remain airborne in the chamber; this will reduce Biosampler efficiency.

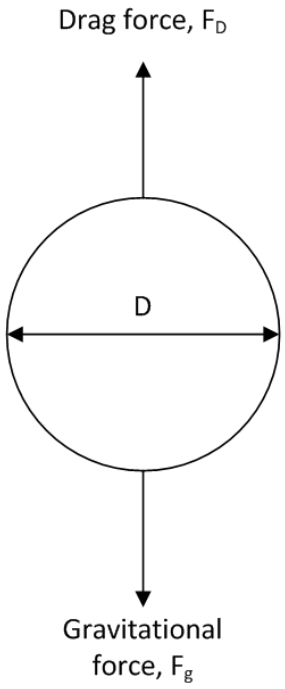

Figure 30. Free body diagram showing the forces acting on a settling particle

Small particles moving at a low velocity through the containment chamber have a small Reynolds number and the flow regime can be assumed to be laminar. In these conditions, the inertial forces are negligible compared to the viscous forces and Stokes' Law can be used to determine the drag force acting on the particle, shown in Equation (4.26) (Cooper & Alley, 2002).

$$F_g = \frac{\pi}{6} \cdot D^3 \cdot \rho \cdot g \tag{4.26}$$

When a particle reaches terminal velocity, the gravitational force (F_g) is equal to the drag force (F_D) acting on the particle as shown in Figure 30. The gravitational force acting on a rigid particle with diameter, D and density, ρ is shown in Equation (4.27).

$$F_D = 3 \cdot \pi \cdot \mu \cdot V \cdot D \tag{4.27}$$

Setting Equations (4.26) and (4.27) together and solving for V, results in the settling velocity of the particle shown in Equation (4.28) (Masters & Ela, 2008).

$$V = \frac{D^2 \cdot \rho \cdot g}{18 \cdot \mu} \tag{4.28}$$

HuNoV particles have a diameter of 32 nm and a buoyant density of 1.41 $\frac{g}{cm^3}$ (Marks et al., 2000). Particles this small undergo random Brownian motion and will eventually collide with other particles and coagulate to form larger particles. Equation (4.29) shows the settling velocity for one single HuNoV particle. This settling velocity is very slow and if uninterrupted, a single virus could remain airborne for a very long time (i.e. multiple years) although it is highly unlikely that a single virus remain uninterrupted and contagious for this length of time.

$$V = \frac{\left(3.2x10^{-9} m\right)^2 \cdot \left(1.41x10^6 \frac{g}{m^3}\right) \cdot \left(9.8 \frac{m}{s^2}\right)}{18 \cdot \left(0.0172 \frac{g}{m \cdot s}\right)} = 4.57x10^{-10} \frac{m}{s} \tag{4.29}$$

A surrogate virus very similar in size to the HuNoV will be used in testing the efficiency of the biosampler system. Surrogate viruses are suspended in a broth or liquid then introduced into the chamber with a collision nebulizer. A BGI, Inc. Collision Nebulizer outputs a particle distribution with a median diameter of 2.5 μm (BGI, 2006). Equation (4.30) shows the settling velocity of a particle with a diameter of 2.5 μm and a density of 1.41x10^6 $\frac{g}{m^3}$.

$$V = \frac{\left(2.5x10^{-6}m\right)^2 \cdot \left(1.41x10^{6}\,\frac{g}{m^3}\right) \cdot \left(9.8\,\frac{m}{s^2}\right)}{18 \cdot \left(0.0172\,\frac{g}{m \cdot s}\right)} = 2.79x10^{-4}\,\frac{m}{s} \tag{4.30}$$

Assuming that this particle was floating around uninterrupted in the containment chamber which is 0.3048 meter high (12 inches), it would take 18 minutes for the particle to settle as shown with Equation (4.31).

$$\tau = \frac{0.3048}{2.79x10^{-4}\,\frac{m}{s}} = 1092.5\ s = 18.2\ mins \tag{4.31}$$

Particles smaller than 2.5 μm inside the chamber would take longer than 18 minutes to settle; settling velocities of particles inside the chamber should be considered when determining the sampling time of the Biosampler.

Conclusions

Using the theory of similitude, a scaled model of the human upper gastrointestinal tract complete with mouth, esophagus and stomach was constructed to simulate projectile vomiting episodes. In later studies, this model will be used together with the containment chamber to test whether it is possible for HuNoV to become aerosolized during a projectile vomiting episode, using a bacteriophage surrogate virus. The containment chamber provides a low infrastructure requirement environment where the vomiting machine can safely and effectively simulate vomiting episodes. Future studies will be able to

characterize the effects of vomiting on the transmission of NoV more effectively by using an accurately scaled vomiting model.

In model construction, the human mouth was represented as a piece of circular tubing without considering the teeth or tongue. During vomiting the upper throat dilates which helps depress the tongue in the mouth. Projectile vomiting episodes expel vomitus at such an extreme force that when vomitus passes over the teeth and tongue, obstruction to the path of vomitus is not anticipated. However, vomiting episodes with low pressures do not produce a forceful expulsion of vomitus and vomitus may pass over the teeth and tongue at a slower speed, which would prompt considering teeth and tongue obstruction. Pressures below 3.33 psi, the minimum pressure used in the stomach chamber as shown in Table 6, were not considered in experimentation because they produced simulated vomiting episodes with little to no expulsion force, resulting in vomitus dripping out the end of the surrogate mouth.

The simulated vomiting device is a convenient model because it has adjustable pressure, vomitus volume, air volume, and head/neck positioning. This device is small enough to be safely operated and maintained inside a laboratory setting. The containment chamber does not include any simulation of air flow (e.g. fan or air conditioning elements) in experimentation. Air flow elements could keep small particles aerosolized for longer periods of time; this model does not address this issue. Since there have not been any clinical studies that examine the aerosolization of viruses during vomiting, it is difficult to validate this experiment at this time. Comparing the results from future clinical studies with the results of future bioaerosolization experiments should be done to support this experiment.

CHAPTER 5: CONCLUSIONS AND RECOMMENDATIONS

Conclusions

At this time, there is limited knowledge on how vomiting affects the airborne transmission of foodborne illnesses. Extensive research was performed to characterize the amount of airborne particles produced during coughing. A preliminary fate model was built using coughing as the primary mechanism for aerosolization of HuNoV particles. The fate model showed that when the mean concentration distribution of airborne HuNoV was $1x10^{10}$, with a standard deviation of 1,000, there is a 95% probability that the number of airborne viruses will be less than or equal to 20. This information is useful because the infectious dose of HuNoV is 10 to 20 infectious viruses (CDC, 2011). When future studies can quantify how vomiting affects the airborne transmission of HuNoV the fate model can be updated by using vomiting as the main aerosolization mechanism rather than coughing. Having a preliminary fate model using coughing is still helpful in determining the combined effect of vomiting and coughing on the aerosolization of HuNoV particles.

Another purpose of the preliminary fate model was to identify key factors that are important as further research efforts focus on building a more robust model. For instance this study recognized that the concentration of HuNoV in vomitus is very important in determining how many HuNoV particles can be aerosolized during coughing after vomiting. There is a lot of uncertainty regarding this quantity in the literature and it merits further research; reducing uncertainty in this quantity will help build a better model for future vomiting mechanism models.

Measurements from the Tipping Bucket experiment suggest that vomitus splatter can be deposited up to 15 ft. away from the initial vomiting location. Results from the Tipping Bucket experiment provide some guidance as to the maximum area that may need to be cleaned and decontaminated after a primary vomiting event. Although the experimental design for this study is somewhat basic, the results can act as a guide, identifying a circular zone with a diameter of up to 30 feet as a conservative estimate for a clean-up area. Disinfection of that area would need to be performed using protocols that would include first cleaning up any vomitus by facility personnel. While wearing protective clothing (e.g. disposable gloves, apron, and face mask) facility personnel would wipe up any vomitus with paper towels and then dispose of the paper towels and waste in a trash bag or biohazard bag. Using soapy water, personnel would wash any surface that came into contact with vomitus while paying special attention to any high-touch surfaces (e.g. door knobs, toilet handles) inside the contamination area. Finally, the surfaces would be rinsed thoroughly with plain water and wiped dry with more paper towels. Once cleaning is complete, facility personnel would then disinfect any hard surfaces affected with at least 1,000 ppm chlorine bleach solution and any porous surfaces affected with a 5,000 ppm chlorine bleach solution (CDC, 2013).

The Tipping Bucket experimental design does not consider the fact that aerosolization of vomitus/virus could occur during vomiting. Aerosolization of virus during vomiting would most likely extend the diameter of contamination far beyond 30 ft., especially in an environment with continuous airflow. To better characterize the phenomenon of virus aerosolization during vomiting, a simulated vomiting model was constructed using the theory

of similitude. The simulated vomiting model, which uses scaled pressures consistent with pressures observed inside the human abdominal cavity during vomiting, is considered a realistic model which can be used to study virus transmission occurring as a consequence of aerosolization during vomiting.

It is imperative to test the efficiency of the containment chamber and biosampler system before experimentation trials. Using Stokes' Law, it was estimated that HuNoV particles could remain airborne in the containment chamber for about 18 minutes under laminar flow conditions. If there is constant circulation inside the containment chamber it is highly likely that HuNoV particles could remain even longer airborne in the chamber. This phenomenon explains why there could be low biosampler efficiencies coupled with low concentrations of HuNoV on swabbed surfaces; this means that a majority of the particles are still airborne and not collected. This is an important scenario to consider when evaluating Biosampler efficiencies.

Recommendations

Further studies quantifying the distances that vomitus splatter can travel should include a method that uses a device to provide forceful projection of the vomitus matrices. Using a device that provides projection of vomitus will produce more realistic conditions for measuring vomitus splatter.

Future studies using the vomiting device to quantify aerosolization of virus from vomiting should consider the following recommendations:

1. The efficiency of the Biosampler/air chamber system should be quantified before experimentation. Using an air collision nebulizer, a known amount of virus can be introduced into the air chamber. Although the Biosampler has a high rated efficiency of capture, it is expected that the amount of airborne virus recovered in the collection vessel will be less than the amount of virus introduced by the nebulizer.
2. A minimum of 10 trials should be completed to quantify efficiency of the Biosampler before aerosolization experiments are conducted.
3. During aerosolization experimentation, the Biosampler should be turned on before a vomiting episode is simulated using the vomiting device. A biosampling time of at least 20 minutes is recommended; this time corresponds to collection volume that is over three times the volume of the air chamber, and is higher than the calculated time (using Stoke's Law) for viruses to remain airborne.
4. Any experimentation using the Biosampler should be corrected for Biosampler efficiency as described in Step 1, to account for any bioaerosols that were not collected by the Biosampler.

REFERENCES

Baker, K., Morris, J., McCarthy, N., Saldana, L., Lowther, J., Collinson, A. & Young, M. (2011). An outbreak of norovirus infection linked to oyster consumption at a UK restaurant, February 2010. *Journal of Public Health*, *33*(2), 205–211. Faculty Public Health.

BGI. (2006). Output Distribution of a Collison Nebulizer.

Caul, E. O. (1994). Small round structured viruses: airborne transmission and hospital control. *The Lancet*, *343*(8908), 1240–1242. Elsevier.

CDC. (2011). Norovirus in Healthcare Facilities Fact Sheet. 1600 Clifton Road, Atlanta, GA.

CDC. (2013). Clean-up and Disinfection for Norovirus ("Stomach Bug").

Cheesbrough, J., Green, J., Gallimore, C., Wright, P., Brown, D. & others. (2000). Widespread environmental contamination with Norwalk-like viruses (NLV) detected in a prolonged hotel outbreak of gastroenteritis. *Epidemiology and infection*, *125*(1), 93–98. Cambridge Univ Press.

Cooper, D. C. & Alley, F. C. (2002). *Air Pollution Control* (3rd. ed.). Waveland Press, Inc.

Dijkstra, P., Hof, A., Stegenga, B. & De Bont, L. (1999). Influence of mandibular length on mouth opening. *Journal of oral rehabilitation*, *26*(2), 117–122. Wiley Online Library.

Duguid, J. (1945). The numbers and the sites of origin of the droplets expelled during expiratory activities. *Edinburgh Medical Journal*, *52*, 385.

Fabian, P., McDevitt, J., Houseman, E. & Milton, D. (2009). Airborne influenza virus detection with four aerosol samplers using molecular and infectivity assays: considerations for a new infectious virus aerosol sampler. *Indoor air*, *19*(5), 433–441. Wiley Online Library.

FMI, F. M. I. (2010). Norovirus Information Guide.

Fox Robert, W., McDonald Alan, T. & Pritchard Philip, J. (2004). Introduction to Fluid Mechanics. Hoboken, NJ: Wiley & Sons, Inc.

Ho, M.-S., Monroe, S., Stine, S., Cubitt, D., Glass, R., Madore, H. P., Pinsky, P., et al. (1989). Viral gastroenteritis aboard a cruise ship. *The Lancet*, *334*(8669), 961–965. Elsevier.

Iqbal, A., Haider, M., Stadlhuber, R. J., Karu, A., Corkill, S. & Filipi, C. J. (2008). A study of intragastric and intravesicular pressure changes during rest, coughing, weight lifting, retching, and vomiting. *Surgical endoscopy*, *22*(12), 2571–2575. Springer.

Johnson, D., Lynch, R., Marshall, C., Mead, K. & Hirst, D. (2013). Aerosol Generation by Modern Flush Toilets. *Aerosol Science and Technology*, (just-accepted). Taylor \& Francis.

Kenneth Koch, M. (2011). Wake Forest School of Medicine.

Keshav, S. (2004). *The gastrointestinal system at a glance* (1st ed.). Blackwell Science Ltd.

Korn, O., Csendes, A., Burdiles, P., Braghetto, I., Sagastume, H. & Biagini, L. (2003). Length of the esophagus in patients with gastroesophageal reflux disease and Barrett's esophagus compared to controls. *Surgery*, *133*(4), 358–363. Elsevier.

Kuo, B. U. D. (2006). Esophagus- anatomy and development. *GI Motility online*.

Lang, I. M., Dana, N., Medda, B. K. & Shaker, R. (2002). Mechanisms of airway protection during retching, vomiting, and swallowing. *American Journal of Physiology-Gastrointestinal and Liver Physiology*, *283*(3), G529–G536. Am Physiological Soc.

Lopman, B., Vennema, H., Kohli, E., Pothier, P., Sanchez, A., Negredo, A., Buesa, J., et al. (2004). Increase in viral gastroenteritis outbreaks in Europe and epidemic spread of new norovirus variant. *The lancet*, *363*(9410), 682–688. Elsevier.

Lumsden, K. & Holden, W. (1969). The act of vomiting in man. *Gut*, *10*(3), 173–179. BMJ Publishing Group Ltd and British Society of Gastroenterology.

Marks, P., Vipond, I., Carlisle, D., Deakin, D., Fey, R. & Caul, E. (2000). Evidence for airborne transmission of Norwalk-like virus (NLV) in a hotel restaurant. *Epidemiology and Infection*, *124*(03), 481–487. Cambridge Univ Press.

Masters, G. M. & Ela, W. P. (2008). *Introduction to Environmental Engineering and Science* (3rd. ed.). Pearson Education, Inc.

Mokhtari, A. & Jaykus, L.-A. (2009). Quantitative exposure model for the transmission of norovirus in retail food preparation. *International journal of food microbiology*, *133*(1), 38–47. Elsevier.

Morawska, L. (2006). Droplet fate in indoor environments, or can we prevent the spread of infection? *Indoor air*, *16*(5), 335–347. Wiley Online Library.

Morawska, L., Hargreaves, M., Ristovski, Z., Guo, H., Corbett, S. & Smith, G. A. (2006). The Impact of the Measuring Method on Droplet Detection From Human Expiration. International Society of Indoor Air Quality and Climate.

Munson, B. R. D. F. Y. & Okiishi, T. H. (2002). Fundamentals of Fluid Mechanics. *John Wiley & Sons, Inc*.

Papineni, R. S. & Rosenthal, F. S. (1997). The size distribution of droplets in the exhaled breath of healthy human subjects. *Journal of Aerosol Medicine*, *10*(2), 105–116.

Scallan, E., Hoekstra, R. M., Angulo, F. J., Tauxe, R. V., Widdowson, M.-A., Roy, S. L., Jones, J. L., et al. (2011). Foodborne illness acquired in the United States—major pathogens. *Emerging infectious diseases*, *17*(1), 7. Centers for Disease Control and

Prevention.

SKC. (2012). Biosampler Operating Instructions. 863 Valley View Road Eighty Four, PA.

Weinstein, R. A., Said, M. A., Perl, T. M. & Sears, C. L. (2008). Gastrointestinal flu: norovirus in health care and long-term care facilities. *Clinical infectious diseases*, *47*(9), 1202–1208. Oxford University Press.

Widdowson, M.-A., Cramer, E. H., Hadley, L., Bresee, J. S., Beard, R. S., Bulens, S. N., Charles, M., et al. (2004). Outbreaks of acute gastroenteritis on cruise ships and on land: identification of a predominant circulating strain of norovirus—United States, 2002. *Journal of Infectious Diseases*, *190*(1), 27–36. Oxford University Press.